

Literature review:

TRADITIONAL AND NEW EMERGING METHODS TO STUDY DRUG
PERMEABILITY AND DRUG-CELL INTERACTIONS IN EARLY PHASES OF
DRUG DISCOVERY

Experimental work:

MONITORING DRUG-CELL INTERACTIONS WITH SURFACE PLASMON
RESONANCE TECHNIQUE

Susanna Hallila
University of Helsinki
Faculty of Pharmacy
Division of Biopharmaceutics
and Pharmacokinetics

March 2013

Tiedekunta – Fakultet – Faculty Faculty of Pharmacy		Osasto – Sektion – Department Biopharmaceutics and Pharmacokinetics	
Tekijä – Författare – Author Susanna Hallila			
Työn nimi – Arbetets titel – Title Literature review: Traditional and new emerging methods to study drug permeability and drug-cell interactions in early phases of drug discovery Experimental study: Monitoring drug-cell interactions with surface plasmon resonance technique			
Oppiaine – Läroämne – Subject Biopharmaceutics			
Työn laji – Arbetets art – Level Master's thesis		Aika – Datum – Month and year March 2013	Sivumäärä – Sidoantal – Number of pages 87
Tiivistelmä – Referat – Abstract <p>There is a strong need for new <i>in vitro</i> methods in early drug development that predict <i>in vivo</i> conditions more reliably. One of the prerequisites for successful drug therapy is sufficient permeability. A drug needs to be transported through a cell membrane before it can have a pharmacological effect. Therefore, the drug-cell interactions are studied in the early stage of the drug development process. The literature review of this work covers the traditional <i>in vitro</i> and <i>in silico</i> methods of predicting the permeability of drugs across the intestinal membrane. The widely applied methods are reviewed briefly and the predictability of the methods is evaluated. Moreover, the surface plasmon resonance (SPR) technique is introduced. The principle of SPR and its applications for predicting intestinal permeability using lipid membranes resembling the intestinal membrane and for studying drug-cell interactions are discussed. The advantage of the SPR technique is that it is an optical method which allows real-time monitoring under a constant flow without labeling agents.</p> <p>The aim of the experimental part of this work was to evaluate the suitability of the SPR technique for cell-based studies to monitor drug-cell interactions in native cellular environments. Previously, the SPR technique has been almost merely used in routine biomolecular interaction analysis. Recently, the SPR technique has also been applied to cell-based assays but in those studies the reason for the SPR signal responses is generally poorly discussed. The objective of the experimental study was to evaluate and optimize different cell culturing approaches for living cell sensing for SPR, i.e. cells immobilized on the roof of the PDMS molded flow channel in the SPR instrument and cells immobilized directly on the SPR sensor surface. ARPE-19 cells were immobilized on the PDMS substrates but the challenge of imaging cell monolayers on PDMS molded SPR flow channels suggested that immobilizing the cells directly on the SPR sensor surface would be a more straightforward procedure. Hence, ARPE-19 and MDCKII cell culturing protocols were optimized for successful immobilization of confluent cell monolayers directly on the SPR sensor surface. However, ARPE-19 cells showed poor resistance against shear stress in the flow channel; whereas MDCKII cells showed much better resistance against shear stress in the flow channel. Therefore, only MDCKII cells immobilized on the SPR sensor surfaces were used for drug-cell interaction studies. After three days of culture MDCKII cells were exposed to test compounds in separate SPR measurements. The used test compounds were propranolol, D-mannitol, D-glucose and HSPC:Chol liposomes. During the SPR measurements, the changes in the SPR peak minimum angular position and SPR peak minimum intensity were recorded in real-time, and these were further used for analysis after the measurements. The results showed that clear differences in both SPR signals between propranolol and D-mannitol were observed when the cells were exposed to the test compounds. Propranolol diffuses effectively by the transcellular pathway into cells whereas D-mannitol uses the paracellular pathway. This indicates that the introduced SPR approach may be a potential <i>in vitro</i> method in order to provide real-time information on the permeability of drugs and possibly on cell uptake mechanisms of nanoparticles for a better mechanistic understanding of drug-cell interactions on a cellular level.</p>			
Avainsanat – Nyckelord – Keywords Surface plasmon resonance, intestinal absorption, MDCKII cells, propranolol, D-mannitol			
Säilytyspaikka – Förvaringställe – Where deposited Department of Biopharmaceutics and Pharmacokinetics			
Muita tietoja – Övriga uppgifter – Additional information Suviseditorit: Manuela Raviña, Tapani Viitala			

Tiedekunta – Fakultet – Faculty Farmasian tiedekunta		Osasto – Sektion – Department Biofarmasia ja farmakokinetiikka	
Tekijä – Författare – Author Susanna Hallila			
Työn nimi – Arbetets titel – Title Kirjallisuuskatsaus: Perinteiset ja uudet menetelmät, joilla tutkitaan lääkeaineen solukalvon läpäisevyyttä sekä lääkeaineen ja solujen välisiä vuorovaikutuksia lääkekehityksen varhaisissa vaiheissa Erikoistyö: Lääkeaineen ja solujen välisten vuorovaikutusten tutkiminen pintaplasmoniresonanssi-tekniikalla			
Oppiaine – Läroämne – Subject Biofarmasia			
Työn laji – Arbetets art – Level Pro Gradu -työ		Aika – Datum – Month and year Maaliskuu 2013	Sivumäärä – Sidoantal – Number of pages 87
Tiivistelmä – Referat – Abstract Lääkekehityksen varhaisiin vaiheisiin tarvitaan uusia, luotettavammin <i>in vivo</i> -tilannetta ennustavia <i>in vitro</i> -tutkimusmenetelmiä. Lääkeaineen täytyy kulkeutua solukalvon läpi ennen kuin se voi päästä vaikutuskohtaansa. Tämän vuoksi lääkeaineen vuorovaikutusta solujen kanssa on tärkeää tutkia lääkekehityksen mahdollisimman varhaisessa vaiheessa. Kirjallisuuskatsauksessa tarkastellaan perinteisiä <i>in vitro</i> ja <i>in silico</i> -menetelmiä, joita käytetään lääkeaineen imeytymisen ennustamiseen ruoansulatuskanavasta. Katsauksessa kuvataan lyhyesti yleisimmin käytettyjä tutkimusmenetelmiä sekä arvioidaan menetelmien luotettavuutta erityisesti lääkeaineen <i>in vivo</i> -imeytymisen ennustamisessa. Lisäksi katsauksessa esitellään uusi pintaplasmoniresonanssi (SPR)-menetelmä ennustamaan lääkeaineen imeytymistä solukalvon läpi. SPR-menetelmää on käytetty muun muassa lääkeaineen imeytymisen tutkimisessa keinoelinten lipidikerrosten avulla sekä lääkeaineen ja solujen välisten vuorovaikutusten tutkimisessa SPR-sensorin pinnalla. SPR-menetelmän etuna on, että sillä on mahdollista tutkia lääkeaineen ja solujen välisiä vuorovaikutuksia reaaliaikaisesti, jatkuvassa virtauksessa ja ilman merkkiaineita. Erikoistyön tavoitteena oli selvittää soveltuuko SPR-menetelmä lääkeaineen ja solujen välisten vuorovaikutusten tutkimiseen. SPR-menetelmää on käytetty aiemmin lähinnä biokemiallisissa tutkimuksissa tarkasteltaessa molekyylien välisiä vuorovaikutuksia. Menetelmällä on tehty myös solututkimuksia, mutta niissä on analysoitu yksinkertaistetusti mitattuja signaalien muutoksia. Erikoistyön tavoitteena oli löytää optimoidut olosuhteet, joissa voitaisiin tehdä SPR-solmittauksia. Tavoitteena oli kasvattaa soluja SPR-laitteen PDMS:lla päällystetyn virtauskanaviston pinnalla tai suoraan SPR-sensorin pinnalla. ARPE-19-solut onnistuttiin kasvattamaan yhtenäisenä solukerroksena PDMS:n pinnalla, mutta solukerroksen tarkastelu PDMS-virtauskanaviston pinnalla oli haastavaa. Tämän vuoksi solut päätettiin kasvattaa SPR-sensorin pinnalla. Viljelyolosuhteet optimoitiin siten, että ARPE-19 ja MDCKII-solut kasvoivat yhtenäisenä solukerroksena SPR-sensorilla. Virtausmittauksissa kuitenkin selvisi, että ARPE-19-solut eivät kestäneet puskurin virtauksen aiheuttamia olosuhteita virtauskanavistossa, kun taas MDCKII-solut kestivät niitä hyvin. Tämän vuoksi varsinaiset SPR-mittaukset tehtiin vain MDCKII-soluilla. Kun MDCKII-soluja oli viljelty kolme päivää SPR-sensorin pinnalla, solukerroksen ja tutkimusaineiden välinen vuorovaikutus mitattiin SPR-laitteella erillisissä mittauksissa. Tutkimusaineina käytettiin propranololia, D-mannitolia, D-glukoosia ja HSPC:KOL-liposomeja. Mittauksissa tarkasteltiin SPR-minimikulman ja SPR-piikin minimi-intensiteetin muutosta reaaliajassa, kun solukerros altistettiin tutkimusaineille. Tulokset osoittivat, että SPR-menetelmällä voitiin havaita selkeä eroavaisuus molemmissa SPR-signaaleissa propranololin ja D-mannitolin välillä. Propranololi läpäisee solukerroksen transsellulaarisesti, kun taas D-mannitoli käyttää parasellulaarista reittiä. Tämä tarkoittaa, että menetelmällä oli mahdollista erottaa nämä imeytymisreitit toisistaan. Tulokset osoittavat, että SPR-tekniikka voi olla potentiaalinen <i>in vitro</i> -menetelmä tutkia lääkeaineiden vuorovaikutuksia solukerroksen kanssa. Menetelmällä olisi mahdollista tutkia esimerkiksi lääkeaineiden ja nanopartikkelien imeytymistä reaaliaikaisesti ja ilman merkkiaineita.			
Avainsanat – Nyckelord – Keywords Pintaplasmoniresonanssi, imeytyminen, MDCKII-solut, propranololi, D-mannitoli			
Säilytyspaikka – Förvaringställe – Where deposited Biofarmasian ja farmakokinetiikan osasto			
Muita tietoja – Övriga uppgifter – Additional information Ohjaajat: Manuela Ravifia, Tapani Viitala			

TRADITIONAL AND NEW EMERGING METHODS TO STUDY DRUG
PERMEABILITY AND DRUG-CELL INTERACTIONS IN EARLY PHASES OF
DRUG DISCOVERY

Susanna Hallila
University of Helsinki
Faculty of Pharmacy
Division of Biopharmaceutics
and Pharmacokinetics

March 2013

CONTENTS

1	INTRODUCTION	1
2	DRUG PERMEABILITY ACROSS INTESTINAL EPITHELIUM.....	3
2.1	Intestinal membrane	3
2.2	Passive diffusion	4
2.3	Carrier-mediated transport	5
2.4	Endocytosis	7
3	METHODS TO PREDICT INTESTINAL PERMEABILITY OF DRUGS.....	7
3.1	<i>In vitro</i> methods	7
3.1.1	Artificial membrane models	7
3.1.2	Cell culture monolayers	9
3.1.3	Surface plasmon resonance technique	11
3.2	<i>In silico</i> methods	12
4	SURFACE PLASMON RESONANCE SPECTROSCOPY	13
4.1	Principle of surface plasmon resonance biosensing	14
4.2	Surface plasmon resonance instrumentation	16
4.3	Biochemical-based assays	17
4.3.1	Functionalization of the sensor surface.....	17
4.3.2	The detection formats	18
4.4	Cell-based assays.....	20
4.4.1	Intracellular reactions induced by stimulation with external agent	22
4.4.2	Toxicity and morphological changes	24
4.4.3	The cell surface binding.....	26
6	CONCLUSIONS.....	26
7	REFERENCES	28

1 INTRODUCTION

A successful drug discovery and development process includes selecting the right disease target, identifying the compound, and executing a functional development process. Absorption, distribution, metabolism, excretion and toxicity (ADME/tox) screening is a major part of the early drug discovery process, where the most suitable drug candidates for the clinic are selected. Drug permeability plays a critical role e.g. in oral absorption, blood-brain barrier permeation, cell-membrane penetration for the intracellular targets and skin absorption of transdermal products. Therefore, permeability has a significant influence on drug absorption and disposition, metabolism and transporter effects, and pharmacokinetics-pharmacodynamics relationships. The permeability is also, along with solubility, the key determinant for the Biopharmaceutical Classification System (BCS) (Amidon et al. 1995).

For orally administered drugs, one of the prerequisites for successful therapy is sufficient intestinal absorption. If the drug candidate has a proven pharmacological effect, but it is absorbed very poorly from the gastrointestinal track, its oral administration is not possible. Therefore, the absorption potential of molecules is studied in the early stage of the drug development process. The prediction is not easy because *in vivo* absorption from the intestine is affected by a great number of factors e.g. the solubility and permeability of a drug, membrane transporters, the integrity of the gastrointestinal tract, presystemic drug metabolism, physiological status and formulation. Various permeability assays have been developed and applied in the drug discovery and development process to predict intestinal absorption, including *in silico*, *in vitro*, *in situ*, and *in vivo* approaches. However, traditional *in vitro* cell assays are often static, time-consuming and laborious. This is particular true for those assays requiring further analytical procedures where the final detection is based on UV spectroscopy, mass spectrometry, or radiometry of labeled compounds. Furthermore, *in situ* and *in vivo* animal experiments are ethically questionable.

Surface plasmon resonance (SPR) is a label-free optical detection instrument which allows real-time monitoring without labeling of the analyte (Kooyman 2008). Usually,

in a traditional SPR application, one of the interacting biomolecules is immobilized on the surface of the gold sensor chip and the analyte is injected onto the chip to detect the interaction between them. This technique has often been used for the analyses of interactions between the analyte and various kinds of biomolecules such as peptides, proteins, nucleic acids, and polysaccharides (Rich and Myszka. 2010; De Crescenzo et al. 2008). SPR has found applications at many stages of the drug discovery process, particularly in ligand discovery and lead optimization (Cooper 2002). It has been used to directly monitor the binding of low molecular weight compounds to immobilized drug targets in order to determine affinity constants and reaction kinetics. Additionally, SPR has been applied in ADME assays to predict absorption by studying the binding of small molecules to liposome surfaces immobilized on the sensor chip surface (Danelian et al. 2000; Cimitan et al. 2005; Frostell-Karlsson et al. 2005). A new emerging application for SPR is the analysis of cellular processes at the whole-cell level where cells are immobilized directly on the sensing surface and stimulated with test compounds (Robelek and Wegener 2010; Chabot et al. 2009; Fujimura et al. 2008).

The literature part of this work focuses on the permeability of drug molecules and reviews the experimental and computational methods that are widely applied to predict the permeability of drugs across the intestinal membrane. The current biosensor and whole-cell applications of the SPR technique are also reviewed in order to clarify the potential of using the SPR technique to study drug-cell interactions, drug absorption routes and cell uptake mechanisms. The experimental part of this work evaluates the suitability of SPR for small molecular drug-cell interactions studies with ARPE-19 and MDCKII cell lines.

2 DRUG PERMEABILITY ACROSS INTESTIAL EPITHELIUM

The oral drug delivery is the most preferred route of drug administration. The oral route is preferred because of its convenience, low costs, and high patient compliance compared to other routes. For orally administered drugs, the amount of drug reaching the blood circulation depends e.g. on the permeability and solubility of a drug, the gastrointestinal pH, gastric emptying, gastrointestinal transit, the presystemic elimination, and the formulation (Barthe et al. 1999). Transport of drug substances across the intestinal membrane is a complex and dynamic process and it may include the passage of compounds across various pathways at the same time. Passive transport takes place through the cell membrane of enterocytes (transcellular) or via the tight junctions between the enterocytes (paracellular). Various influx and efflux transporters can also be functional during absorption. This chapter focuses on the permeability of the drugs across the intestinal membrane.

2.1 Intestinal membrane

Approximately 90% of all absorption in the gastrointestinal track occurs in the small intestinal region (Balimane and Chong 2005). The anatomy and physiology of the intestinal membrane have a major impact on the absorption process. The physiological role of the small intestine is the selective absorption of nutrients and to serve as a barrier to digestive enzymes and ingested foreign substances. The length of the human small intestine is approximately 2-6 m. It is divided into duodenum, jejunum and ileum which comprise 5%, 50%, and 45% of the length. There is microvillus on the surface of the intestine, which greatly increases the surface area available for absorption. The intestinal membrane consists of enterocytes, goblet cells that secrete mucin, endocrine cells, paneth cells, M cells, tuft, and cup cells. The absorption occurs mostly across enterocytes. The enterocytes are polarized cells which are separated by tight junctions.

2.2 Passive diffusion

The cellular membrane is a lipid bilayer composed of various amphiphilic phospholipids, cholesterol and proteins (Sugano et al. 2010). It forms a thin, (approximately 5 nm) hydrophobic barrier which separates the cell interior from the extracellular aqueous environment. Passive diffusion is a concentration gradient-driven mass transport of compound across the cell membrane which is not consuming energy (ATP). Passive diffusion follows Fick's law, whereby the absorption rate is proportional to the drug concentration and the surface area. Passive diffusion can be divided into transcellular or paracellular processes, as shown in Figure 1. Transcellular diffusion through a membrane occurs across the lipid bilayer of enterocytes. The center of the lipid bilayer is highly hydrophobic; therefore a compound diffuses across lipid bilayer mainly as an uncharged molecule. Transcellular transport generally depends on the uncharged fraction of the compound defined by the pK_a of the molecule and the physicochemical properties of the molecule, such as lipophilicity ($\log P/\log D$), polar surface area, hydrogen bond number and molecular size.

Passive paracellular diffusion in the intestine occurs via the tight junctions between the cells (Figure 1). The molecules with molecular weight approximately <200 g/mol may use this transport route (Fagerholm et al. 1999). For larger molecules, it is considered as a minor transport route because of the limited intercellular space. The available surface area for paracellular intestinal absorption has been estimated to be approximately as low as 0.01% of the total surface area of the small intestine (Madara and Pappenheimer 1987). However, paracellular transport may be an important absorption mechanism for hydrophilic drugs that have poor membrane permeability and that are not transported via intestinal uptake carriers.

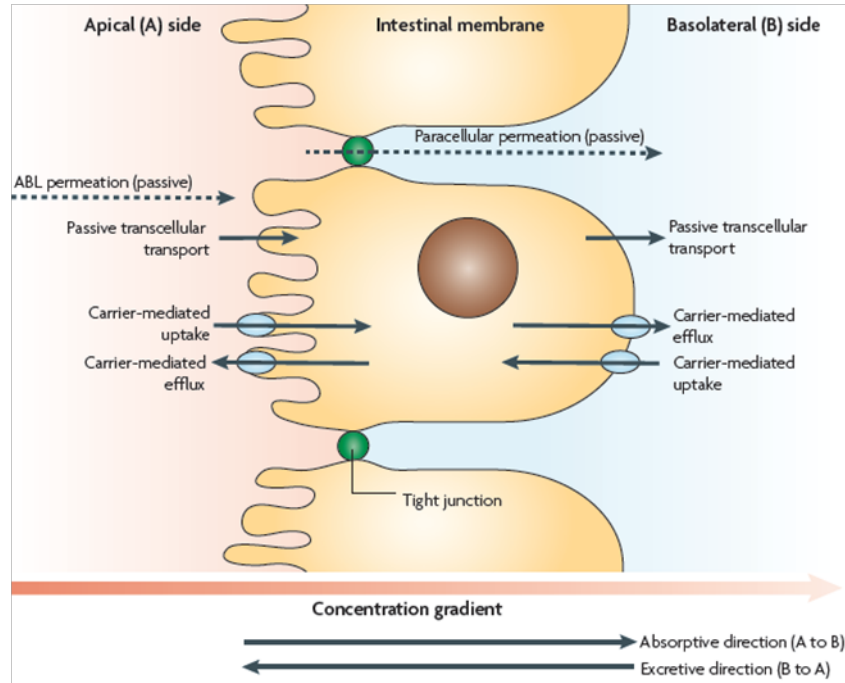


Figure 1. Transport mechanisms through the intestinal membrane (Sugano et al. 2010).

2.3 Carrier-mediated transport

Carrier-mediated transport of drugs occurs through specific cells that express the transporter and the binding is stereospecific, and often enantioselective (Sugano et al. 2010). When the transport process directly or indirectly consumes energy (ATP), the transport process is active and does not require any concentration gradient of the compound. Carrier-mediated transport occurs via transporters, which can transport drugs into (influx) a cell or out of a cell (efflux). In the case of primary active transport, transporters require binding and the hydrolysis of ATP to operate. While in the case of secondary active transport, transporters are driven by ion gradients created by ATP-dependent primary transporters, such as Na^+/K^+ -ATPase. However, carrier-mediated transport can also occur passively and is then driven by the concentration of the substrate (facilitated transport). The carrier-mediated transport is saturable. The saturation occurs when the total number of molecules exceeds the number of carrier protein binding sites available for transport.

There are more than 400 membrane transporters in humans (Giacomini et al. 2010). Two major superfamilies are the ATP-binding cassette (ABC) and the solute carrier (SLC) families. The clinically significant uptake and efflux transporters of the drugs in the intestinal membrane are shown in Figure 2. If the drug is a substrate of a transporter, it is translocated across a membrane by the transporter. An inhibitor of a drug transporter can decrease the influx and/or efflux of the drug competitively or non-competitively, whereas an inductor of a drug transporter can increase the transport. The carrier-mediated transport via uptake transporters is a crucial absorption mechanism for some drugs, but it can also cause clinically significant interactions between drugs.

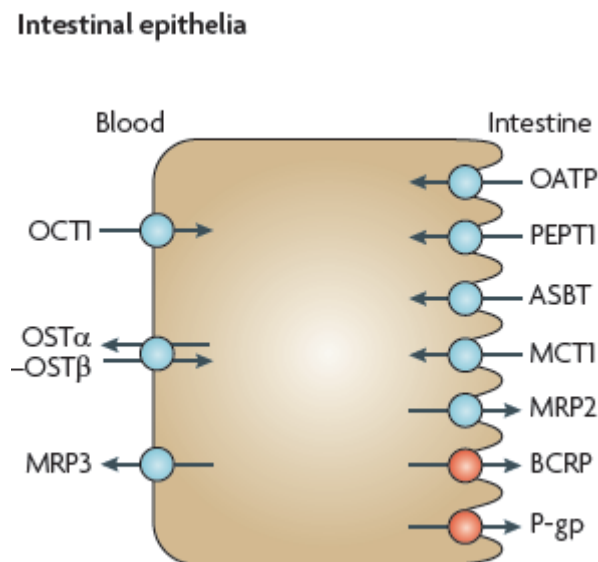


Figure 2. Most important transporters in the intestinal epithelia. There are several uptake receptors in the apical membrane of the enterocyte including transporters of the organic anion transporting polypeptide (OATP) family, peptide transporter 1 (PEPT1), ileal apical sodium/bile acid co-transporter (ASBT) and monocarboxylic acid transporter 1 (MCT1). The efflux transporters include multidrug resistance protein 2 (MRP2), breast cancer resistance protein (BCRP) and P-glycoprotein (P-gp). The basolateral membrane contains organic cation transporter 1 (OCT1), heteromeric organic solute transporter (OST α -OST β) and MRP3 (Edited from Giacomini et al. 2010).

2.4 Endocytosis

Endocytosis is an uptake mechanism for the uptake of macromolecules, which is consuming energy (Conner and Schmid 2003). In endocytosis, macromolecules are transported into the cell in membrane-bound vesicles derived from the cell membrane. Endocytosis may occur via phagocytosis or pinocytosis, but phagocytosis is typically restricted to specialized cells, including macrophages, monocytes and neutrophils. However, pinocytosis occurs in all cells by multiple mechanisms: macropinocytosis, clathrin-mediated endocytosis, caveolae-mediated endocytosis, and clathrin- and caveolae-independent endocytosis. Nanoparticles and large peptides may be absorbed by the intestinal epithelium via endocytosis (Anderson et al. 2001; Gao et al. 2011). Therefore, nanoparticle mediated drug delivery systems may be effective for enhancing the intestinal absorption of the drugs that have a low oral bioavailability.

3 METHODS TO PREDICT INTESTINAL PERMEABILITY OF DRUGS

Several permeability assays have been developed and applied in the drug discovery and development process to predict intestinal absorption, including *in silico*, *in vitro*, *in situ*, and *in vivo* approaches. This chapter reviews relatively rapid *in vitro* and *in silico* methods that are used in the early drug discovery process for the prediction of intestinal permeability of lead compounds in humans.

3.1 *In vitro* methods

3.1.1 Artificial membrane models

In 1998, Kansy et al. introduced the parallel artificial membrane permeability assay (PAMPA) to predict transcellular absorption of drugs in the intestine. PAMPA is based on a 96-well microtiter plate technology, where the plate is covered with a microtiter filter plate in a sandwich construction. Each composite well is divided into a donor and an acceptor chamber, which are separated by a hydrophobic permeability filter. The

lipid membrane is formed on the filter and the flux factors between a donor and an acceptor compartments are measured. The membrane is completely artificial without any paracellular pathway and active transporters. Therefore, only the human absorption of transcellularly transported compounds can be predicted reliably.

During the past decade, several enhanced variants of PAMPA have been developed by different researchers, including differences in membrane composition, solution composition, and hydrodynamics. First Kansy and co-workers used (1998) a lipid barrier formed by a mixture of egg-lecithin and *n*-dodecane. Later the composition of the lipid membrane has been varied e.g. to dioleoyl phosphatidylcholine in dodecane, and *n*-hexadecane alone to develop even faster, simpler and a more robust method to predict passive, transcellular permeability (Avdeef et al. 2001; Wohnsland and Faller 2001). Avdeef et al. (2004) introduced a modification of PAMPA where stirring of the donor compartment was used. The stirring decreased permeation time of lipophilic drugs significantly and allowed faster analyses. The double-sink PAMPA method was also introduced by Avdeef et al. (2005) to stimulate the transit. In this method, the donor compartment consisted of pH gradient “sink” for acids and lipophilic gradient “sink” for bases in acceptor compartment and also an individual-well magnetic stirring mechanism.

PAMPA is a simple and fast physicochemical method in order to predict passive transcellular permeability of compounds (Kansy et al. 1998; Avdeef et al. 2007). The advantage of this method is a higher throughput and relatively lower cost compared to cell-based permeability assays. Due to the ability of screening thousands of compounds a day, PAMPA is a useful tool in the early phase of drug discovery to screen the libraries in order to predict passive oral absorption. Moreover, PAMPA can provide information on the lipophilicity, the ionization state, and the solubility of a compound. As in cellular models, a significant unstirred water layer may exist within the PAMPA model. Without stirring, the thickness of the unstirred water layer has been estimated to vary from approximately 2000 to 4000 μm , but a value as low as 300 μm have been shown when plates were lightly shaken (Wohnsland and Faller 2001; Avdeef et al. 2004). The thickness is thought to be <100 μm *in vivo* (Levitt et al. 1990). Thick

unstirred water layer can represent the rate-limiting step for determining permeation for poorly soluble lipophilic drugs, thus complicating the predictability of *in vivo* permeability.

3.1.2 Cell culture monolayers

In vitro experiments using cultured cell monolayers are one of the most often applied methods in order to estimate the intestinal absorption of drug candidates in the preclinical phase. The cells are grown on semi-permeable filters to form monolayers, which morphologically resemble the intestinal epithelium (Irvine et al. 1999). The monolayers are grown on filter supports and the passage of a drug from the apical to the basolateral compartment and the basolateral to the apical is measured. Unlike lipid-based artificial membrane models, cell culture-based models have structural and biological properties characteristic of differentiated intestinal epithelia. Because cells express various drug transporters and metabolic enzymes, the models have the capability to study permeability properties other than just passive transcellular diffusion (Seithel et al 2006). However, there are also a number of disadvantages in the models. Several factors can induce the assay variability such as culture time, seeding density, passage number, and culture conditions, and those can affect cellular properties (Volpe 2008). In addition, the extensive culture times before assays makes the cell-based permeability studies laborious with high costs.

Human colon carcinoma (Caco-2) cell monolayer model is widely used as a tool for evaluating human intestinal permeability (Press and Di Grandi 2008). Caco-2 cells differentiate spontaneously structurally and functionally into a cell monolayer with polarization that has functions similar to intestinal enterocytes (Hidalgo et al. 1989). Furthermore, they express similar drug transporters as the human small intestine, but the expression of the most well-known drug transporters is lower in Caco-2 cells than in human enterocytes (Seithel et al. 2006). A qualitative relationship between *in vitro* Caco-2 cellular transport and *in vivo* drug permeability has been established by several researchers (Lennernäs et al. 1996; Irvine et al. 1999; Skolnik et al. 2010). In 1996, Lennernäs et al. observed that drugs with rapid and complete passive transcellular

transport had comparable permeability between Caco-2 cells and *in vivo* human jejunum. However, the uptake was observed to be lower in Caco-2 cells, when the tested compounds were using the paracellular pathway or carrier-mediated uptake transport. Thus, the Caco-2 assay has been shown to be more predictive of human absorption for certain classes of drugs than others because of differences in the paracellular radius and transporter expression. The disadvantage the performance of the absorption studies with this cell line is also a relatively low high-throughput capability due to the 3-weeks culture period resulting in high costs. Therefore, a 96-well Caco-2 assay has been developed in order to achieve higher throughput permeability assessment with cells (Skolnik et al. 2010; Mariano et al. 2005). It should be noted that the results from Caco-2 cell permeability assays can exhibit significant inter-laboratory variability, because of differences in cell source, passage number and culture conditions (Hayeshi et al. 2008). Even small differences in the culture conditions may have a significant impact on transporter expression in Caco-2 cells.

The Madin-Darby canine kidney (MDCK) epithelial cell line has been used in permeability assays because of its faster maturation time in culture compared to Caco-2 cells (Irvine et al. 1999). MDCK cells form a columnar epithelium and tight junctions when cultured on semi-permeable membranes. Although the cell line is derived from the renal epithelia of a canine, it has been reported that permeability results from MDCK cells are similar to permeability results from Caco-2 cells for passively absorbed drugs. In addition, MDCK cells have a relatively low expression of drug transporters making it suitable for the prediction of passive absorption (Braun et al. 2000). However, for better prediction for permeability MDCKII-LE (low efflux) cell line has been developed having fivefold lower canine P-glycoprotein protein level than MDCKII-WT (Di et al. 2011). This cell line may provide benefits over MDCKII-WT with less background transporter signals and less probability of interference from canine P-glycoprotein.

3.1.3 Surface plasmon resonance technique

The SPR technique has already been used in the pioneering studies of drug interactions with lipid membranes resembling the intestinal membrane for predicting intestinal permeability (Danelian et al. 2000; Cimitan et al. 2005; Frostell-Karlsson et al. 2005). Liposomes are captured on a sensor chip to create a lipid barrier representative of an intestinal epithelial cell. The stagnant aqueous layer next to the lipid surface mimics the unstirred water layer of the intestinal mucosa. Then the interactions between drugs and immobilized liposomes are monitored by SPR without the need for intrinsic or extrinsic labeling agents. The interaction is measured in real-time and not only binding level but also interaction kinetics are monitored directly.

Danelian et al. (2000) applied SPR in order to study the interactions between 27 compounds and liposomes immobilized on the sensor chip. The results from SPR measurements were compared to reliable estimates for the drug fraction absorbed from the intestine (F_a) in human. The results revealed that the SPR technique can be used to predict F_a in humans for drugs using the transcellular absorption route. Later in 2005, the interactions between 78 drug compounds and immobilized liposomes were studied (Frostell-Karlsson et al. 2005). Based on these results, it was possible to divide the compounds into groups of high, medium, or low level of absorption. Moreover, SPR has been successfully applied to predict the interaction between drugs and the intestinal surface using a sensor chip on which brush border membrane vesicles from a rat were immobilized (Kim et al. 2004; Kim et al. 2005). The results of these studies demonstrated that immobilized brush border membrane surfaces on the sensor chip closely mimic the surface of the small intestine in human. Kim et al. (2004) found that the method provided important information that predicts F_a in humans for transcellularly absorbed drugs.

It has been suggested that the SPR based assay could be used prior to other more complex screens to eliminate compounds that are likely to show low absorption *in vivo* (Frostell-Karlsson et al. 2005; Kim et al. 2004). The SPR based assay predicts only passive absorption, because active transport routes and enzymes are not expressed.

Certainly, the influence of active transporters needs to be measured with specific transporter assays. However, the SPR based assay could also be beneficial to use along with other *in vitro* data to predict whether the rate-determining step in the absorption of a compound will be due to transporter affinity as opposed to membrane affinity. In addition, the interaction between a drug and liposome can be investigated under a wide range of conditions that mimic various *in vivo* membrane environments e.g. under different hydrodynamic flow conditions, which directly reflects the unstirred water layer thickness (Baird et al. 2002).

3.2 *In silico* methods

Numerous computational structure-based models to predict passive intestinal absorption have been published (Hou et al. 2006). The attempt is to establish a relationship between different molecular properties and the absorption in humans. The most widely used computational approach to the coarse estimation of passive intestinal absorption is “rule of 5” proposed by Lipinski and coworkers in 1997 from the analysis of 2245 drugs from the World Drug Index. It presents that poor absorption is more probable for compounds with molecular weight > 500 Da, calculated LogP >5, a number of hydrogen donors >5 and number of hydrogen bond acceptors >10. The rule can only be used to rapidly distinguish between well-absorbed molecules and poorly-absorbed molecules, and therefore it has been necessary to develop prediction models for specific absorption properties.

Most computational prediction methods applied in the estimation of drug absorption are using data modeling (Hou et al. 2006). Data modeling can be applied with great efficiency to a large number of compounds, but it requires a significant quantity of high quality data to deduce a relationship between the structures and the modeled property. Therefore, the reliability and applicability of a computational model is highly dependent on the quality of the dataset used during model development. Typically, models applied to predict intestinal absorption, are quantitative structure-property relationship (QSPR) models which are based on appropriate descriptors. QSPR modeling is developed from simple multiple linear regression to modern multivariate analysis techniques or

machine-learning methods. Many important physicochemical descriptors are introduced into the prediction of drug absorption, such as polar surface area, lipophilicity parameters ($\log P$, $\log D$), molecular weight, and the number of hydrogen bond acceptors and donors. However, it is not possible to determine drug absorption by a single defined descriptor, but rather by the combination of different physicochemical descriptors.

Several QSAR approaches have been proposed to predict human intestinal absorption and Caco-2 cell permeability (Gozalbes et al. 2011; Suenderhauf et al. 2011; Wessel et al. 1998). Linnankoski et al. (2008) demonstrated that computationally derived mathematical models can predict with a reasonable accuracy human passive absorption, when models were compared to cell lines, artificial membrane models, and *in vivo* rat experiments. The results showed that three of seven models were found to be significantly more reliable in predicting human passive intestinal absorption than the artificial membrane models. Two of the models were found to be as reliable as the Caco-2 and 2/4/A1 cell lines. Moreover, one of the computational models even predicted the absorption of drugs nearly as well as absorption studies on rats. Therefore, the simple computational models with high throughput are particularly useful tools in the early screening of drug candidates to predict intestinal passive absorption.

4 SURFACE PLASMON RESONANCE SPECTROSCOPY

SPR-based biosensing is one of the most advanced label-free, real-time detection techniques. The first application of SPR for gas detection and biosensing was demonstrated in 1983 by Liedberg and coworkers. Today, SPR is employed in important applications in food safety, biology, medical diagnostics, and drug discovery (Copeer 2002; Homola 2008). This chapter focuses on the principle of the SPR method and cell-based SPR applications that have been applied so far.

4.1 Principle of surface plasmon resonance biosensing

SPR spectroscopy is an optical method, which measures the change in the refractive index on a surface of metal (Kooyman 2008). The detection principle relies on an electron charge density wave phenomenon that occurs on the surface of a metallic film when light is reflected at the film under particular conditions. The first demonstration of optical excitation was made by Otto, Kretschmann and Raether (Kretschmann and Raether 1968; Otto 1968). A typical experimental set-up of the SPR measurement using the so called Kretschmann configuration is shown in Figure 3.

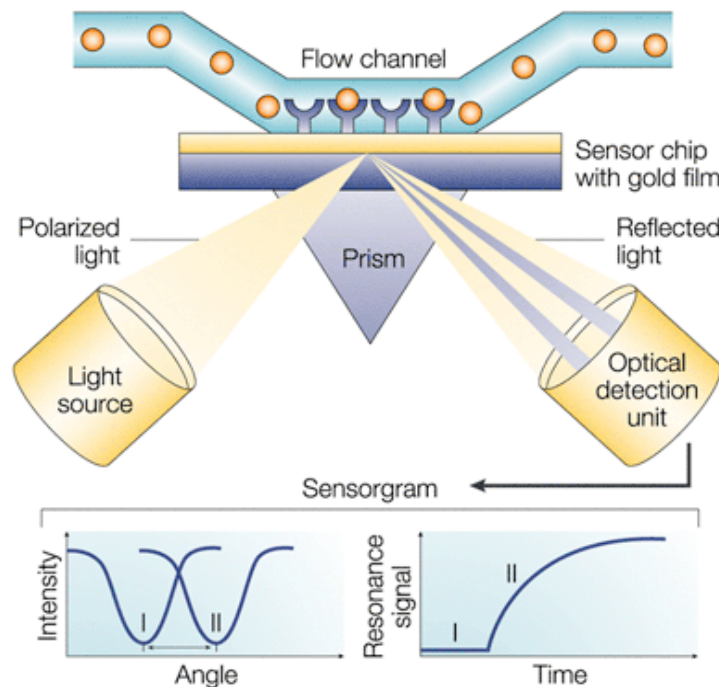


Figure 3. The principle of SPR detection using the conventional Kretschmann optical configuration. SPR detects changes in the refractive index in the immediate vicinity of the sensor surface. It appears as a sharp dip in the reflected light from the surface at an angle that is dependent on the mass of molecules on the surface (left bottom image). The SPR angle shifts when molecules bind to the surface and mass on the surface is changed. The change is monitored by plotting the resonance angle signal versus time in a so called sensorgram (right bottom image) (Cooper 2002).

The evanescent wave is essential in the concept of SPR sensing (Kooyman 2008). The refraction of the evanescent wave at the interface between two media with refractive indexes n_1 and n_2 follows Snell's law (equation 1). The equation reveals the direction of light after refraction.

$$\frac{n_1}{n_2} = \frac{\sin\theta_2}{\sin\theta_1} \quad (1)$$

When p-polarized light is directed at an interface between a metal and a dielectric material, Fresnel's equations reveal how much of the light is refracted and how much is reflected (Kooyman 2008). The complex reflection coefficient r_p for p-polarized incident light electric field in the interface between two media is defined by the Fresnel equation:

$$r_p = \frac{E_i}{E_r} = |r_p| e^{i\varphi} = \left| \frac{\tan(\alpha - \beta)}{\tan(\alpha + \beta)} \right| e^{i\varphi} \quad (2)$$

where E_i and E_r are the incident and reflected electric fields, respectively, and the angle α is the incident angle and β the angle of refraction. Surface plasmons are charge-density oscillations occurring at the interface between a metal and a dielectric. The wave vector of the surface plasmon wave (K_{sp}) is defined by equation 3:

$$K_{sp} = \frac{\omega}{c} \sqrt{\frac{\epsilon_M n_D}{\epsilon_M + n_D}} \quad (3)$$

where ω is the angular frequency, c the speed of the light, ϵ_M the metal permittivity and n_D the dielectric refractive index. A coupling method between the prism or grating, and the metal surface is required for surface plasmon resonance to occur (Figure 3). The coupling matches the wavevectors of the incident light and the surface plasmons enabling the electromagnetic field component of the p-polarized light to penetrate to the metal layer and transferring energy to the free electrons on the metal surface. This energy transfer produces surface plasmons at the metal-dielectric interface. As a result of the energy transfer, the coupling appears as a sharp dip in the measured reflectance as a function of a specific angle of incidence which is illustrated in Figure 3 (left bottom image). The reflection at the metal-dielectric interface generates an evanescent field in both the metal and the dielectric media propagating approximately 300 nm into the

dielectric media. When the prism refractive index and the laser wavelength are kept constant, the conditions for maximum coupling will change with a modification of the medium refractive index, which is caused for example by the adsorption and desorption of molecules on the surface. As a summary, when a molecule absorbs or binds to the gold surface, the local refractive index change leads to a change in the SPR signal. The size of the change in SPR signal is directly proportional to the mass immobilized onto the surface. The SPR signal measured usually is the SPR peak minimum position (angle or wavelength) or the intensity change at a fixed angle near the minimum of the SPR peak depending on the SPR instrument used.

4.2 Surface plasmon resonance instrumentation

SPR instruments contain at least three integrated components: SPR instrumental optics, a liquid handling system and a sensor chip (Schasfoort and McWhirter 2008). The properties of the gold sensor chip have a vital influence on the quality of the measurements. The gold sensor chip is a physical barrier between the dry optical unit and the wet flow channel. Instruments differ in performance based on differences in optical systems and a degree of development and automation. The optical systems with prism, gratings and optical waveguides are applied to excite surface plasmons. In prism configuration, also called the Kretschmann configuration, a prism couples p-polarized light in to the gold film and reflects the light on a light intensity detecting device using a photodiode or a camera. The Kretschmann configuration can be further divided into fan-shaped beam, fixed angle and angle scanning SPR instruments. In a grating coupler, light is reflected at the lower refractive index substrate, whereas some instruments have optical waveguide couplers where the shift of SPR wavelength is followed. All configurations are measuring the change of refractive index directly, in real-time and without any labels.

Three major liquid handling systems are the flow channels, the cuvette and the microfluidic chip (Schasfoort and McWhirter 2008). Peristaltic or syringe pumps are used to pump the liquid onto the sensor surface, whereas the samples are transported by syringes or peristaltic pumps with or without pneumatic valves and sample loops. Some

instruments have an automatic injection system and some are applied manually. The flow channels are formed when microfluidic channels are pressed against the sensor chip. The planar flow channels are mostly employed in SPR instruments and confined wall-jet flow channels and hydrodynamic flow channels are less common. A planar flow channel is comprised of a single broad channel with an inlet and outlet, from which liquid flows and interacts with the sensor surface. The cuvette liquid handling system is formed by an open container which is manually or automatically filled with liquid. The cuvette is placed on the sensor surface and reactions occur at the bottom of the cuvette. The cuvette requires a mixing system in order to gain more reliable sensorgrams. The disadvantage of the cuvette system is its open architecture which allows the evaporation of the sample solution.

4.3 Biochemical-based assays

4.3.1 Functionalization of the sensor surface

Usually, a sensor chip is functionalized for SPR measurements by attaching one of the interacting molecules, biorecognition element or target molecule, onto the surface of the sensor surface (Homola et al. 2008). Which of the molecules is immobilized depends on the used sensing scheme. In direct, sandwich, and competitive assay, the biorecognition element is immobilized, but in the inhibition assay the immobilized molecule is the target molecule or its derivate. The detection formats are reviewed in detail in the next section (4.3.2). The choice between biorecognition element and an immobilization method is critical because it is affecting the performance of the assay such as sensitivity, specificity, and the limit of detection.

The interacting molecules can be immobilized either on a surface of the sensor chip or in a three-dimensional matrix. The main approaches for immobilizing of molecules to the sensor surface are based on physical, covalent or bioaffinity immobilization (Koubova et al. 2001; Busse et al. 2002; Lee et al. 2005). The covalent immobilization strategies include chemical reactions such as amine, aldehyde or thiol coupling (Löfås et al. 1995). Self-assembled monolayers (SAMs) of alkanethiols or disulfides have been

widely used for a covalent immobilization of biomolecules (Lahiri et al. 1999; Lee et al. 2005). SAMs of oligo(ethylene glycol)-tethered molecules are used to reduce a non-specific binding of molecules on the sensing surface (Zareie et al. 2008). Also polymeric layers such as carboxylated dextran can be used for covalent binding (Löfås et al. 1995). It has been shown that there is no difference in binding kinetics between SAMs and a dextran hydrogel (Lahiri et al. 1999). Another approach for the immobilizing the biorecognition element is based on biochemical affinity reactions using the biotin/streptavidin system (Busse et al. 2002). In this method, the protein streptavidin is immobilized on the gold surface providing binding sites for a subsequent attachment of biotin-conjugated protein. Clearly, the selection of the functionalization strategy is mainly application driven.

4.3.2 The detection formats

Biochemical assays performed with SPR can be divided into four different sensing schemes that are typically applied. Those are direct assays, sandwich assays, competitive assays, and inhibition assays (Figure 4). With a direct binding assay format the interaction between a receptor and an analyte is investigated (Homola et al. 2002). In a direct assay a receptor of a medium- and large-molecular weight molecule is chemically bonded to the gold surface of the SPR sensor chip (Figure 4A). Macromolecules bind to the immobilized receptors which produces a local increase in the refractive index. This increase in the refractive index is measured and can be correlated to the amount of captured analyte. However, the direct assay is only useful for the detection of large molecules because small molecules have often a too low mass to produce a measurable change in the refractive index. Homola and coworkers (2002) used a direct assay in SPR measurements for detection of staphylococcal enterotoxin B in milk, and the SPR was shown to be capable of directly detecting concentrations of staphylococcal enterotoxin B in a buffer as low as 5 ng/ml.

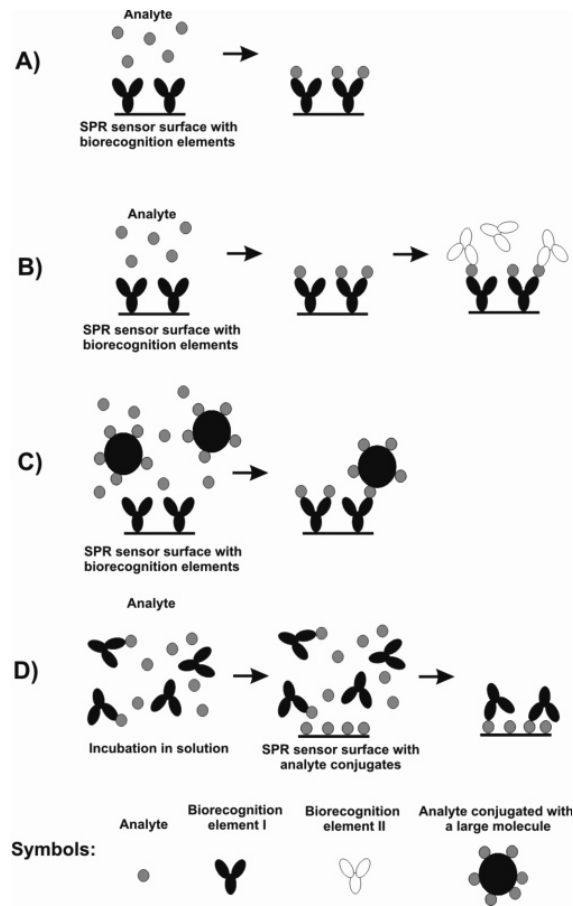


Figure 4. Main sensing schemas used in SPR bioassays: (A) direct assay, (B) sandwich assay, (C) competitive assay, and (D) inhibition assay (Edited from Homola 2008).

A sandwich assay consists of two steps (Figure 4B) (Homola et al. 2002). First the antibody is immobilized onto the sensor chip following the binding of the analyte. In the second step, a secondary antibody is injected over the sensing surface in order to bind to the earlier captured analyte. This format is used to enhance sensitivity and specificity. In addition to the direct assay, the sandwich assay was also used in Homola's et al. study to amplify a sensor response and verify the binding of the analyte. The detection limit of 0,5 ng/ml of staphylococcal enterotoxin B both in milk and buffer was achieved. The detection limit was 10-fold lower than in the direct detection assay. Yao and coworkers (2006) used the sandwich assay in order to analyze oligonucleotide and polynucleotide samples with low concentrations by utilizing gold nanoparticles to enhance the SPR signal. For the analysis of a 39-mer target DNA, the detection limit was in the femtomolar range and the amount of sample needed per analysis was only 15 μ l.

The competitive assay is based on two samples (Figure 4C) (Shimomura et al. 2001). In one sample the small analyte is free and in another it is conjugated to a larger protein. Both samples are competing for the same recognition molecules immobilized on the SPR sensor surface. In this method, the decrease in the signal is proportional to the amount of target sample. The concentration of the conjugated sample is known while the concentration of the free sample is unknown. Shimomura and his research group developed a rapid method in order to quantify endocrine disrupting chemicals, 2,3,7,8-TCDD, polychlorinated biphenyls, and atrazine, from the buffer using a competitive assay. The competitive method was performed because low-molecular-weight analytes did not give any SPR signal in a direct assay, thus binding to the antibody was not observed. However, the detection limit of all test compounds was between 0,1-5 ng/ml using the competitive method.

In the inhibition assay, an analyte or its analogue is immobilized on the sensor surface (Figure 4D) (Fitzpatrick and O’Kennedy 2004). A fixed concentration of an antibody with affinity to an analyte is mixed with a sample containing an unknown concentration of the analyte and then, the mixture is injected to the sensing surface. The binding of the unreacted antibodies is measured as they bind to the analyte molecules immobilized on the sensor surface and therefore the sensor response is inversely proportional to the concentration of the free analyte in the solution. Fitzpatrick and O’Kennedy (2004) used the inhibition assay in order to detect physiologically active a nonprotein-bound fraction of warfarin in plasma ultrafiltrate. The assay precision range was approximately 4-250 ng/ml, which is within the clinical range.

4.4 Cell-based assays

A new emerging application for SPR is the analysis of cellular processes at the whole-cell level (Hide et al. 2002). The SPR technique provides a non-invasive method in order to investigate cellular responses in living cells in real-time. In 2002, Hide et al. suggested that SPR might have the capacity to detect a variety of cellular responses. Since then, several applications have been introduced where SPR have been used to examine a diverse array of cellular processes with various types of cells (Fujimura et al.

2008; Chabot et al. 2009; Chen et al. 2010). In those applications, the cells were cultured directly on the gold sensor chip followed by the stimulation with an external agent and cell responses were analyzed by using reflectance or angular change information. The real-time monitoring of cellular activation is possible by SPR because the stimulation often induces morphological changes, such as a cell contraction and spreading. These changes should affect the basal portion of the cell, which lies within the evanescent field of the surface plasmon (Figure 5). The evanescent field on the surface is approximately 300 nm, while the thickness of a cell is several μm :s, meaning that only the bottom portion of cells can be sensed by SPR. The other approach introduced is the application where an analyte is immobilized on the gold sensor chip while suspension of intact cells is introduced on the surface (Mizuguchi 2012). This approach can only be applied to detect specific ligand-receptor interactions. This section reviews the cell-based SPR studies where cells are immobilized directly on the gold sensor chip.

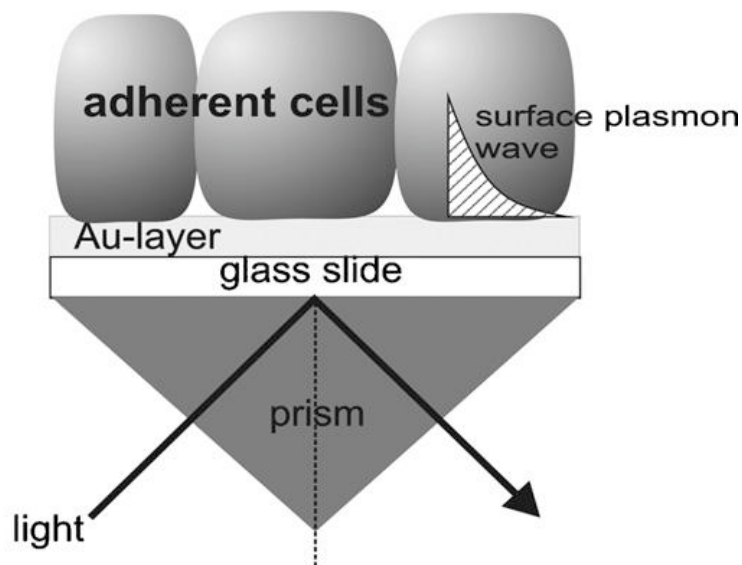


Figure 5. Schematic diagram of SPR sensor immobilized with cells with a Kretschmann configuration (Edited from Robelek and Wegener 2010).

4.4.1 Intracellular reactions induced by stimulation with external agent

In 2002, Hide et al. first introduced that SPR can be applied to the analysis of interactions between living cells and molecules reactive to the cells, using mast cells and mast-cell reactive antigens. The IgE-sensitized mast cells were immobilized on the gold sensor chip and stimulated by an antigen. The exposure of the antigen to the immobilized cells induced a robust and long-lasting increase of the SPR angle in a dose dependent manner. The maximal increase in the SPR angle induced by the antigen was approximately 1000 times higher than the theoretically expected increase for the simple binding of the antigen to the receptor. These results suggest that SPR can detect intracellular signaling, and not just simple binding kinetics between the receptor on the cell surface and their ligands. Tanaka et al. (2008) studied in detail the molecular events that are responsible for a major change in the SPR angle, when RBL-2H3 mast cells were stimulated with the antigen, by using the genetic manipulation of intracellular signaling molecules. The SPR analysis was done by immobilizing the cells overexpressing and/or having a defect in the intracellular signaling molecules on the gold sensor chip followed by the stimulation with the antigen. The results indicated that the antigen-induced increase of the SPR angle in RBL-2H3 cells is greatly dependent on the activation of spleen tyrosine kinase, a linker for activation of T cells, Grb2-related adaptor protein and protein kinase C.

Yanase et al. (2007a) investigated the relationship between the area of cell adhesion to a gold sensor chip and the change of SPR angle using SPR technique. RBL-2H3 rat mast cells and PAM212 mouse keratinocytes were cultured directly on the gold sensor chips. The results showed that the shift of the SPR angle was proportional to the cell density of non-stimulated cells on the gold sensor chip. The cells were stimulated with either antigen or epidermal growth factor causing great changes in the SPR angle with both compounds. However, the results were not consistent with the studied relationship between the change of SPR angle and adherent cell number. Based on the SPR results and microscopic visualization, it was suggested that the change in the SPR angle induced by extracellular stimuli reflects intracellular events rather than changes in the size of the area where cells adhere.

Later in 2007, Yanase et al. (2007b) demonstrated that SPR can also detect the reactions of non-adherent cells, including human basophils and lymphocytes, by fixing them to the gold sensor chip. Three types of fixing methods were tested, a biocompatible anchor for cell membranes, aminoalkanethiol and an amino-reactive cross-linker. All three methods were capable of fixing cells on the gold sensor chip. The study showed that SPR was able to detect cell activation in spheroid cells, when cells were stimulated with antigens. The activation was observed as a change in the SPR angle. This indicates that the SPR technique may be a useful tool for the analysis of clinically important cell functions, such as basophil histamine-release, and lymphocyte stimulation.

In 2010, a new method was introduced for the evaluation of G protein-coupled receptor (GPCR) activation utilizing the SPR technique (Chen et al. 2010). Chinese hamster ovary (CHO)-K1 cells expressing GPCRs were cultured directly on a gold sensor chip and stimulated with GPCR ligands. They succeeded in monitoring GPCR-mediated cellular responses in cells by using SPR. The results suggest that the GPCR-mediated actin rearrangement in the cellular cortex in the evanescent field is reflected in the SPR responses. The study indicates that the SPR analysis may be useful in ligand/drug discovery for certain types of receptors when cytoskeletal rearrangements are involved.

Moreover, Lee and his group (2006) have applied SPR to study interactions between ligand and GPCRs using living cells. HEK-293 cells expressing olfactory receptors (ODR-10) on the cell surface were cultured on a poly-D-lysine coated gold sensor chip. When the cells were exposed to known specific receptor-agonist, it resulted in an SPR angle change in a dose-dependent manner. The cells without ORD-1 receptors did not show any response in the SPR angle. The activation of the cells expressing the receptor by the agonist induced an increase in the intracellular Ca^{2+} ions, which resulted in a change in the SPR angle. The supposed increase of intracellular Ca^{2+} was confirmed by measuring the cytosolic Ca^{2+} ions.

4.4.2 Toxicity and morphological changes

Chabot et al. (2009) showed that the SPR technique could be applied to study a large variety of cellular responses involving to shape remodeling induced by external agents. Human embryonic kidney-293 (HEK-293) cells were grown on a gold sensor chip. The immobilized cells were monitored when the cells were stimulated with three types of stimuli: a bacterial endotoxin (lipopolysaccharides), a chemical toxin (sodium azide) and a physiological agonist (thrombin). The fixed angle intensity decreased after stimulation of lipopolysaccharides and an increase in the concentration lead to an increase in the magnitude of the measured SPR response. The result was confirmed by phase contrast micrographs, which indicated a collapse of the intracellular structure after 30 min of stimulation. Stimulation with sodium azide also decreased the measured signal and micrographs showed an increase in the size of the intracellular space as a result of cell shrinkage. When cells were stimulated with thrombin, the SPR signal was first decreasing followed by a slower recovery back to the baseline. Microscopic observations confirmed that this was due to cell contraction followed by with respreading of the cells. The results showed that SPR can be used to monitor real-time morphological changes in the cells induced by chemical or biological agents. The study demonstrated the possibility to utilize SPR biosensor for environmental and health care applications to determine the presence of toxins and their corresponding cellular responses and in pharmacological studies to better understand cell signaling pathways activated by pharmacological agents.

Cuerrier and coworkers (2008) also applied the SPR technique to study morphological changes in living cells induced by an external agent. They used SPR to quantify the cellular activity of an epithelial cell monolayer stimulated by angiotensin II. HEK-293 cells, stably expressing the angiotensin II AT₁ receptor, were cultured on the gold sensor chip. Immediately after the stimulation by angiotensin II, a rapid decrease in the fixed angle intensity was observed about 2 min after stimulation followed by an increase in the fixed angle intensity that gradually exceeded the baseline value. The same response was not observed, when cells were pretreated with AT₁ receptor antagonist. Microscopic visualization revealed that after 2 min after the cell stimulation

with angiotensin II, a contraction of the cell body was clearly visible with an increase in the intercellular spaces compared to the observations before analysis. This initial cell response was followed by a spreading of the cells and a decrease of the intercellular spaces. Confocal micrographs revealed a temporal redistribution of actin after angiotensin II stimulation, which was also found to be consistent with the SPR signal variation. The study demonstrates that morphological changes in a human epithelial cell monolayer can be followed in real-time using the SPR technique.

Recently, the interaction between monoclonal antibody EGFR1 and membrane protein epidermal growth factor receptor (EGFR) on human gastric cancer BGC823 cells has been studied using the SPR technique (Liu et al. 2011). When immobilized cells were stimulated with EGFR1, the fixed angle intensity first shifted to a higher value and later declined gradually. Microscopic visualization revealed that after the stimulation the shapes of most cells changed from fusiform to round confirming that EGFR1 causes changes in cells' morphology. It was observed that the higher the concentration of EGFR1, the greater the fraction of rounded cells and the higher the decrease in the observed reflection intensity. The results proposed that EGFR1 might lead to the cytoskeletal rearrangements, reduce cells' adhesion forces, and influence living BGC823 cells' survival properties. This study also demonstrated that the SPR technique is capable of real-time detection of molecular interactions and cellular responses in living cells.

SPR has also been applied to detect volume changes in cells which are directly grown on the gold sensor chip (Robelek and Wegener 2010). MDCKII cells were grown as a confluent monolayer on the surface. When a hypertonic buffer was flowed over the cells, it was observed that a rapid increase in the fixed angle intensity took place, while a hypotonic buffer decreased the signal. It was assumed that the stimulation with the hypertonic buffer increased the signal because of the loss of cellular water from the cytosol causing an increased cytoplasmic concentration of intracellular osmolytes which increased a refractive index in the evanescent field. Recently, Baumgarten and Robelek (2011) studied the volume responses of two renal epithelial cell types to non-isotonic

challenges with SPR. These studies showed that the SPR approach might be extended to a platform technology to screen for the therapeutic modulators of cell volume changes.

4.4.3 The cell surface binding

SPR analysis has been used to study the structure-activity relationship between major green tea catechins and their corresponding epimers (Fujimura et al. 2008). The cell-surface binding of catechins to the cell surface and 67 kDa laminin receptor (67LR) was observed by SPR. Basophilic KU812 cells were immobilized on the surface of the SPR sensor chip and the cell-surface binding of eight kinds of tea catechins was studied. Differences in the fixed angle intensity were observed when galloylated catechins were bound to the surface of KU812 cells, but their non-galloylated forms did not induce any signal changes. The binding strengths of catechins in the SPR analysis suggested which functional groups are essential for the cell surface-binding of the catechins. Involvement of the 67LR in the cell-surface binding of galloylated catechins was studied with 67LR-downregulated KU812 cells. The SPR measurement revealed that the cell-surface binding of all galloylated catechins was inhibited by the knockdown of 67LR expression. These patterns were also observed in the inhibitory effects of histamine release in a fluorometric assay. The results indicate that SPR analysis may be suitable for cell studies in order to study the binding of compounds to the cell surface or to specific cell surface receptors.

6 CONCLUSIONS

The permeability of a drug is crucial for the absorption and distribution of the drug. The oral delivery is the main administration route of drugs. Therefore various *in vitro* and *in silico* permeability assays have been developed and applied in the early phases of drug discovery and development process to predict intestinal absorption. The aim is to identify the pharmacologically active drug candidates which have the most promising ADME properties for the lead optimization and finally for clinical trials. However, traditional *in vitro* cell assays are often static, time-consuming, laborious, and suffer

from the influence of the unstirred water layer thickness, which reduces the predictability of *in vivo* permeability especially for lipophilic compounds. Other *in vitro* assays e.g. PAMPA and *in silico* methods are suitable for high-throughput screening but these techniques only predict passive absorption, and do not take account other possible routes, e.g. paracellular or active transport.

SPR is a non-invasive optical technique, which does not require labeling agents. In addition, it is a highly sensitive method enabling real-time monitoring of reactions in the immediate vicinity of a sensor surface. SPR technique is suitable for semi high-throughput screening and only low amount of compounds is needed. Several studies have demonstrated that SPR may be beneficial for the study of the permeability of drugs in the early phases of drug discovery but so far the intestinal permeability has been predicted with SPR by liposome-based *in vitro* systems to study passive absorption. However, SPR has also been applied in the cell-based assays, where cells are immobilized directly on the sensor surface. Several studies indicate that it is possible to monitor real-time intracellular reactions induced by external agents by SPR. These studies suggest that SPR may be utilized for the prediction of ADME properties, e.g. the intestinal absorption of drug candidates. Depending on the cell line immobilized on the sensor surface, not only passive but also the active transport of compounds may be studied. The SPR cell-based method could be beneficial to be used along with other *in vitro* methods in order to predict intestinal drug absorption in the lead optimization phases of drug discovery, because it provides complementary data for traditional assays which could help in a better mechanistic understanding of drug absorption and drug-cell interactions. However, although SPR seems like a promising tool for drug absorption and drug-cell interactions studies, it is good to keep in mind that the phenomena detected by SPR are often very complex processes that might be difficult to interpret. Therefore, it is foreseen that a thorough validation of the SPR approach for drug absorption and drug-cell interaction studies against traditional assay is needed before it possibly will be widely accepted by pharmaceutical scientists for pharmaceutical research.

7 REFERENCES

- Amidon GL, Lennernäs H, Shah VP, Crison JR: A theoretical basis for a biopharmaceutical drug classification: The correlation of *in vitro* drug product dissolution and *in vivo* bioavailability. *Pharmaceut Res* 12: 413–420, 1995
- Anderson KE, Eliot LA, Stevenson BR, Rogers JA: Formulation and evaluation of a folic acid receptor-targeted oral vancomycin liposomal dosage form. *Pharmaceut Res* 18: 316-322, 2001
- Artursson P: Epithelial transport of drugs in cell-culture. I: A model for studying the passive diffusion of drugs over intestinal absorptive (Caco-2) cells. *J Pharm Sci* 79: 476-482, 1990
- Avdeef A, Strafford M, Block E, Balogh MP, Chambliss W, Khan I: Drug absorption in vitro model: filter-immobilized artificial membranes: 2. Studies of the permeability properties of lactones in *Piper methysticum* Forst. *Eur J Pharm Sci* 14: 271–280, 2001
- Avdeef A, Nielsen PE, Tsinman O: PAMPA—a drug absorption in vitro model 11. Matching the *in vivo* unstirred water layer thickness by individual-well stirring in microtitre plates. *Eur J Pharm Sci* 22: 365-374, 2004
- Avdeef A, Artursson P, Neuhoff S, Lazorovab L, Gråsjö J, Tavelin S: Caco-2 permeability of weakly basic drugs predicted with the Double-Sink PAMPA pK^{flux}_a method. *Eur J Pharm Sci* 24: 333–349, 2005
- Avdeef A, Bendels S, Di L, Faller B, Kansy M, Sugano K, Yamauchi Y: PAMPA - Critical factors for better predictions of absorption. *J Pharm Sci* 96: 2893-2909, 2007
- Baird CL, Courtenay ES, Myszka DG: Surface plasmon resonance characterization of drug/liposome interactions. *Anal Biochem* 310: 93-99, 2002
- Balimane PV, Chong S: Cell culture-based models for intestinal permeability: a critique. *Drug discov today* 10: 335-343, 2005
- Barry P, Di Grandi D: Permeability for intestinal absorption: Caco-2 assay and related issues. *Curr Drug Metab* 9: 893-900, 2008
- Barthe L, Woodley J, Houin G: Gastrointestinal absorption of drugs: methods and studies. *Fundam Clin Pharm* 13: 154-168, 1999
- Baumgarten S, Robelek R: Surface plasmon resonance (SPR) sensors for the rapid, sensitive detection of the cellular response to osmotic stress. *Sensor Actuat B-Chem* 156: 798-804, 2011
- Braun A, Hämmerle S, Suda K, Rothen-Rutishauser B, Gunthert M, Krämer SD, Wunderli-Allenspach H: Cell cultures as tools in biopharmacy. *Eur J Pharm Sci* 11: S51-S60, 2000

Busse S, Scheumann V, Menges B, Mittler S: Sensitivity studies for specific binding reactions using the biotin/streptavidin system by evanescent optical methods. *Biosens Bioelectron* 17: 704-710, 2002

Carlsson R, Engvall E, Freeman A, Ruoslahti E: Laminin and fibronectin in cell adhesion: Enhanced adhesion of cells from regenerating liver to laminin. *Proc Natl Acad Sci USA* 78: 2403-2406, 1981

Chabot V, Cuerrier CM, Escher E, Aimez V, Grandbois M, Charette PG: Biosensing based on surface plasmon resonance and living cells. *Biosens Bioelectron* 24: 1667-1673, 2009

Chen K, Obinata H, Izumi T: Detection of G protein-coupled receptor-mediated cellular response involved in cytoskeletal rearrangement using surface plasmon resonance. *Biosens Bioelectron* 25: 1675-1680, 2010

Cimitan S, Lindgren MT, Bertucci C, Danielson UH: Early absorption and distribution analysis of antitumor and anti-AIDS drugs: Lipid membrane and plasma protein interactions. *J Med Chem* 48: 3536-3546, 2005

Conner SD, Schmid SL: Regulated portals of entry into the cell. *Nature* 422: 37-44, 2003

Cooper MA: Optical biosensors in drug discovery. *Nat Rev Drug Discov* 1: 515-528, 2002

Cuerrier CM, Chabot V, Vigneux S, Aimez V, Escher E, Gobeil F, Charette PG, Grandbois M: Surface plasmon resonance monitoring of cell monolayer integrity: Implication of signaling pathways involved in actin-driven morphological remodeling. *Cell Mol Bioeng* 1: 229-239, 2008

Danelian E, Karlen A, Karlsson R, Winiwarter S, Hansson A, Löfås S, Lennernäs H, Hämäläinen MD: SPR biosensor studies of the direct interaction between 27 drugs and a liposome surface: Correlation with fraction absorbed in humans. *J Med Chem* 43: 2083-2086, 2000

De Crescenzo G, Boucher C, Durocher Y, Jolicoeur M: Kinetic characterization by surface plasmon resonance-based biosensors: Principle and emerging trends. *Cell Mol Bioeng* 1: 204-215, 2008

Di L, Whitney-Pickett C, Umland JP, Zhang H, Zhang X, Gebhard DF, Lai Y, Federico JJ, Davidson RE, Smith R, Reyner EL, Lee C, Feng B, Rotter C, Varma M, Kempshall S, Fenner K, El-Kattan AF, Liston TE, Troutman MD: Development of a new permeability assay using low-efflux MDCKII cells. *J Pharm Sci* 100: 4974-4985, 2011

Fagerholm U, Nilsson D, Knutson L, Lennernäs H: Jejunal permeability in humans in vivo and rats in situ: investigation of molecular size selectivity and solvent drag. *Acta Physiol Scand* 165: 315-324, 1999

Fitzpatrick B, O’Kennedy R: The development and application of a surface plasmon resonance-based inhibition immunoassay for the determination of warfarin in plasma ultrafiltrate. *J Immunol Methods* 291: 11–25, 2004

Frostell-Karlsson Åsa, Widegren H, Green CE, Hämäläinen MD, Westerlund L, Karlsson R, Fenner K, Van De Waterbeemd H: Biosensor analysis of the interaction between drug compounds and liposomes of different properties; a Two-Dimensional characterization tool for estimation of membrane absorption. *J Pharm Sci* 94: 25-37, 2005

Fujimura Y, Umeda D, Yamada K, Tachiban H: The impact of the 67 kDa laminin receptor on both cell-surface binding and anti-allergic action of tea catechins. *Arch Biochem Biophys* 476: 133–138, 2008

Gao F, Zhang Z, Bu H, Huang Y, Gao Z, Shen J, Zhao C, Li Y: Nanoemulsion improves the oral absorption of candesartan cilexetil in rats: Performance and mechanism. *J Control Release* 149: 168-174, 2011

Giacomini KM, Huang SM, Tweedie DJ et al: Membrane transporters in drug development. *Nature* 9: 215-236, 2010

Gozalbes R, Jacewicz M, Annand R, Tsaïoun K, Pineda-Lucena A: QSAR-based permeability model for drug-like compounds. *Bioorgan Med Chem* 19: 2615-2624, 2011

Hayeshi R, Hilgendorf C, Artursson P, Augustijns P, Brodin P, Dehertogh P, Fisher K, Fossati L, Hovenkamp E, Korjamo T, Masungi C, Maubon N, Mols R, Müllertz A, Mönkkönen J, O’Driscoll C, Oppers-Tiemissen HM, Ragnarsson EGE, Rooseboom M, Ungell AL: Comparison of drug transporter gene expression and functionality in Caco-2 cells from 10 different laboratories. *Eur J Pharm Sci* 35: 383-396, 2008

Hidalgo IJ, Raub TJ, Borchardt RT: Characterization of the human colon carcinoma cell line (Caco-2) as a model system for intestinal epithelial permeability. *Gastroenterology* 96: 736-749, 1989

Hide M, Tsutsui T, Sato H, Nishimura T, Morimoto K, Yamamoto S, Yoshizato K: Real-time analysis of ligand-induced cell surface and intracellular reactions of living mast cells using a surface plasmon resonance-based biosensor. *Anal Biochem* 302: 28-37, 2002

Homola J, Dostálek J, Chen S, Rasooly A, Jiang S, Yee SS: Spectral surface plasmon resonance biosensor for detection of staphylococcal enterotoxin B in milk. *Int J Food Microbiol* 75: 61– 69, 2002

Homola J: Present and future of surface plasmon resonance biosensors. *Anal Bioanal Chem* 377: 528–539, 2003

Homola J: Surface plasmon resonance sensors for detection of chemical and biological species. *Chem Rev* 108: 462-493, 2008

Hou T, Wang J, Zhang W, Wang W, Xu X: Recent advances in computational prediction of drug absorption and permeability in drug discovery. *Curr Med Chem* 13: 2653–2667, 2006

Irvine JD, Takahashi L, Lockhart K, Cheong J, Tolan JW, Selick HE, Grove JR: MDCK (Madin-Darby canine kidney) cells: A tool for membrane permeability screening. *J Pharm Sci* 88: 28-33, 1999

Kansy M, Senner F, Gubernator K, 1998: Physicochemical high throughput screening: parallel artificial membrane permeation assay in the description of passive absorption processes. *J Med Chem* 41: 1007–1010, 1998

Kim K, Cho S, Park JH, Byun Y, Chung H, Kwon IC, Jeong SY: Surface Plasmon resonance studies of the direct interaction between a drug/intestinal brush border membrane. *Pharmaceut Res* 21: 1233-1239, 2004

Kim SK, Kim K, Lee S, Park K, Park JH, Kwon IC, Choi K, Kimd CY, Byun Y: Evaluation of absorption of heparin-DOCA conjugates on the intestinal wall using a surface plasmon resonance. *J Pharm Biomed* 39: 861-870, 2005

Kooyman RPH: Physics of surface plasmon resonance. *Handbook of Surface Plasmon Resonance*, p.15-34, Edited by Schasfoort RBM, Tudos AJ, The Royal society of Chemistry, Cambridge 2008

Koubova V, Brynda E, Karasova L, Skvor J, Homola J, Dostalek J, Tobiska P, Rosicky J: Detection of foodborne pathogens using surface plasmon resonance biosensors. *Sens Actuators B* 74: 100-105, 2001

Kretschmann E, Raether H: Radioactive decay of non radiative surface plasmons excited by light. *Z Naturforsch A* 23: 2135, 1968

Lahiri J, Isaacs L, Tien J, Whitesides GM: A strategy for the generation of surfaces presenting ligands for studies of binding based on an active ester as a common reactive intermediate: A surface plasmon resonance study. *Anal Chem* 71: 777-790, 1999

Lee JW, Sima SJ, Choa SM, Lee J: Characterization of a self-assembled monolayer of thiol on a gold surface and the fabrication of a biosensor chip based on surface plasmon resonance for detecting anti-GAD antibody. *Biosens Bioelectron* 20: 1422-1427, 2005

Lee JY, Ko HJ, Lee SH, Park TH: Cell-based measurement of odorant molecules using surface plasmon resonance. *Enzyme Microb Tech* 39: 375-380, 2006
Lennernäs H, Palm K, Fagerholm U, Artursson P: Comparison between active and passive drug transport in human intestinal epithelial (Caco-2) cells *in vitro* and human jejunum *in vivo*. *Int J Pharm* 127: 103–107, 1996

Levitt MD, Fume JK, Strocchi A, Anderson BW, Levitt DG: Physiological measurements of luminal stirring in the dog and human small bowel. *J Clin Invest* 86: 1540-1547, 1990

Liedberg B, Nylander C, Lundström I: Surface plasmon resonance for gas detection and biosensing. *Sensor Actuator* 4: 299-304, 1983

Linnankoski J, Ranta VP, Yliperttula M, Urtti A: Passive oral drug absorption can be predicted more reliably by experimental than computational models - Fact or myth. *Eur J Pharm Sci* 34: 129-139, 2008

Lipinski CA, Lombardo F, Dominy BW, Feeney PJ: Experimental and computational approaches to estimate solubility and permeability in drug discovery and development settings. *Adv Drug Deliv Rev* 23: 3-25, 1997

Liu F, Zhang J, Den Y, Wang D, Lu Y, Yu X: Detection of EGFR on living human gastric cancer BGC823 cells using surface plasmon resonance phase sensing. *Sensors Actuat B-Chem* 153: 398-403, 2011

Marino AM, Yarde M, Patel H, Chong S, Balimane PV: Validation of the 96 well Caco-2 cell culture model for high throughput permeability assessment of discovery compounds. *Int J Pharm* 297: 235-241, 2005

Mizuguchi T, Uchimura H, Kataoka H, Akaji K, Kiso Y, Saito K: Intact-cell-based surface plasmon resonance measurements for ligand affinity evaluation of a membrane receptor. *Anal Biochem* 420: 185-187, 2012

Otto A: Excitation of nonradiative surface plasma waves in silver by the method of frustrated total reflection. *Z Phys* 216: 398-410, 1968

Pattnaik P: Surface plasmon resonance: Applications in understanding receptor-ligand interaction. *Appl Biochem Biotech* 126: 79-92, 2005

Rich RL, Myszka DG: Grading the commercial optical biosensor literature - Class of 2008: 'The Mighty Binders'. *J Mol Recognit* 23: 1-64, 2010

Robelek R, Wegener J: Label-free and time-resolved measurements of cell volume changes by surface plasmon resonance (SPR) spectroscopy. *Biosens Bioelectron* 25: 1221-1224, 2010

Schasfoort RMB, McWhirter A: SPR instrumentation. *Handbook of Surface Plasmon Resonance*, p.34-78, Edited by Schasfoort RBM, Tudos AJ, The Royal society of Chemistry, Cambridge 2008

Seithel A, Karlsson J, Hilgendorf C, Björquist A, Ungell, AL: Variability in mRNA expression of ABC- and SCL-transporters in human intestinal cells: comparison between human segments and Caco-2 cells. *Eur. J. Pharm. Sci.* 28: 291-9, 2006

- Shimomura M, Nomura Y, Zhang W, Sakino M, Lee KH, Ikebukuro K, Karube I: Simple and rapid detection method using surface plasmon resonance for dioxins, polychlorinated biphenyls and atrazine. *Analytica Chimica Acta* 434: 223–230, 2001
- Skolnik S, Lin X, Wang J, Chen XH, He T, Zhang B: Towards prediction of *in vivo* intestinal absorption using a 96-Well Caco-2 assay. *J Pharm Sci* 99: 3246–3265, 2010
- Suenderhauf C, Hammann F, Maunz A, Helma C, Huwyler J: Combinatorial QSAR modeling of human intestinal absorption. *Mol Pharm* 8: 213-24, 2011
- Sugano K, Kansy M, Artursson P, Avdeef A, Bendels S, Di L, Ecker GF, Faller B, Fischer H, Gerebtzoff G, Lennernäs H, Senner F: Coexistence of passive and carrier-mediated processes in drug transport. *Nat rev Drug discovery* 9: 597-614, 2010
- Tanaka M, Hiragun T, Tsutsui T, Yanase Y, Suzuki H, Hide M: Surface plasmon resonance biosensor detects the downstream events of active PKC β in antigen-stimulated mast cells. *Biosens Bioelectron* 23: 1652-1658, 2008
- Volpe DA: Variability in Caco-2 and MDCK cell-based intestinal permeability assays. *J Pharm Sci* 97: 712-725, 2008
- Wessel MD, Jurs PJ, Tolan JW, Muskal SM: Prediction of human intestinal absorption of drug compounds from molecular structure. *J Chem Inf Comput Sci* 38: 726-735, 1998
- Yao X, Li X, Toledo F, Zurita-Lopez C, Gutova M, Momand J, Zhou F: Sub-attomole oligonucleotide and p53 cDNA determinations via a high-resolution surface plasmon resonance combined with oligonucleotide-capped gold nanoparticle signal amplification. *Anal Biochem* 354: 220–228, 2006
- Yanase Y, Suzuki H, Tsutsui T, Hiragun T, Kameyoshi Y, Hide M: The SPR signal in living cells reflects changes other than the area of adhesion and the formation of cell constructions. *Biosens Bioelectron* 22: 1081–1086, 2007a
- Yanase Y, Suzuki H, Tsutsui T, Uechi I, Hiragun T, Mihara S, Hide M: Living cell positioning on the surface of gold film for SPR analysis. *Biosens Bioelectron* 23: 562-567, 2007b
- Zareie HM, Boyer C, Bulmus V, Nateghi E, Davis TP: Temperature-responsive self-assembled monolayers of oligo(ethylene glycol): Control of biomolecular recognition. *ACS Nano* 2: 757-65, 2008

MONITORING DRUG-CELL INTERACTIONS WITH SURFACE PLASMON
RESONANCE TECHNIQUE

Susanna Hallila
University of Helsinki
Faculty of Pharmacy
Division of Biopharmaceutics
and Pharmacokinetics

March 2013

CONTENTS

1	INTRODUCTION	1
2	AIM OF THE STUDY.....	2
3	MATERIALS AND METHODS.....	4
3.1	Cell culture	4
3.2	Immobilization of cells on the flow channel of SPR biosensor	4
3.2.1	Preparation of PDMS substrates	4
3.2.2	Modification of PDMS substrates.....	5
3.2.3	Culturing of ARPE-19 cells on PDMS substrates	6
3.3	Culturing of cells on surface plasmon resonance gold sensor chips	7
3.3.1	Modification of gold sensor chips.....	7
3.3.2	Immobilization of cells on gold sensor chip.....	7
3.4	Viability of cells on PDMS substrates and gold sensor chips.....	8
3.4.1	Trypan blue test.....	8
3.4.2	MTT assay	8
3.5	Flow experiments with the immobilizer.....	9
3.6	Test compounds in surface plasmon resonance analysis	10
3.7	Surface plasmon resonance analysis	11
3.8	Data handling	12
4	RESULTS	13
4.1	Attachment and proliferation of ARPE-19 cells on PDMS substrates.....	13
4.2	Growing and viability of the cells on gold sensor chip.....	17
4.2.1	ARPE-19 cells.....	18
4.2.2	MDCKII cells.....	20
4.3	Flow experiments	23
4.4	Drug-cell interaction analysis with surface plasmon resonance	26
5	DISCUSSION	34
5.1	Growing of the cells on PDMS substrates	34
5.2	Growing and viability of the cells on gold sensor chip.....	35
5.3	Resistance of cells to buffer flow.....	37
5.4	Surface plasmon resonance in living cell sensing.....	37
6	CONCLUSIONS.....	43
7	REFERENCES	44

1 INTRODUCTION

There is a strong need for new complementary *in vitro* methodologies for preclinical phases of the drug discovery and development process. The aim is to speed up the drug development process, to build a better understanding of drug absorption and drug-cell interactions, and to find, develop and optimize different administration routes. This is true, particularly in the case of nanoparticle mediated and liposomal drug delivery. Especially, the ability of examining living cells in their native and physiological relevant environments is crucial in order to improve the mechanistic understanding during drug discovery and development. Although cell-based assays are less specific and more complex than biochemical assays, cell-based assays give functional information that would otherwise be lost with biochemical assays. However, traditional *in vitro* cell assays, which are widely applied during preclinical phases, are laborious and static. Moreover, most of those assays measure a specific cellular event and the labeling of the ligand or target with a fluorescent compound is needed for imaging or detection purposes. Thus, the optical biosensors may offer a potential cell-based assay that can provide noninvasive and continuous data from cellular activity with high sensitivity.

For the past 20 years, optical biosensors have been almost merely applied for routine biomolecular interaction analysis because of their capabilities to provide detailed information on the binding affinity and kinetics of an interaction (Rich and Myszka. 2010; De Crescenzo et al. 2008). In particular, the ability to directly detect the binding of small molecules to immobilized receptors has widely increased the utility of optical biosensors in drug screening (Hämäläinen et al. 2000). Recently, optical biosensors have also been applied for cell-based assays because optical biosensors can screen and characterize a wide variety of cellular activity in native cellular environments without labeling (Fang 2011). Label-free cell-based assays based on an optical biosensor detection may have the potential to be utilized in many phases during the drug development process, including hit selection and optimization, screening of the

absorption, distribution, metabolism, excretion and toxicity (ADME/Tox) properties of drug candidates.

Among the label-free techniques developed for probing the activities and interactions of living cells, the surface plasmon resonance (SPR) technique has been widely used. SPR is a non-invasive optical detection technique that does not require labeling agents (Kooyman 2008). Moreover, SPR is a highly surface sensitive method and it enables real-time monitoring. The SPR technique is based on surface plasmons which are longitudinal charge density waves occurring at the interface between a thin metal film such as gold or silver and the surrounding medium. The evanescent field of the surface plasmon extends approximately 300 nm into the surrounding medium meaning that only the basal portion of the cell layer is sensed by the SPR technique. However, several studies have demonstrated that SPR is a powerful tool in real-time and non-labeled monitoring of living cells for studying diverse arrays of cellular processes (Yanase et al. 2007; Fujimura et al. 2008; Chabot et al. 2009). The detection in these cell-based assays is based on the knowledge that cellular activation with an external agent often results in cellular reorganization, such as mass distribution, cell contraction and spreading, which affects the basal portion of the immobilized cells within the evanescent field.

2 AIM OF THE STUDY

The aim of this study was to evaluate the suitability of the SPR technique for cell-based studies to monitor drug-cell interactions in native cellular environments. SPR spectroscopy is an optical method which measures the change in the refractive index at the gold surface (Kooyman 2008). Briefly, when a compound adsorbs or binds to the gold sensor chip, the local refractive index changes leads to a change in the SPR angle which can be monitored in real-time. The size of the change in the SPR signal is directly proportional to the mass of the compound adsorbed or immobilized onto the gold sensor chip surface. The aim of this study was to immobilize cells either directly on the gold sensor chips or on the roof of the flow channel (Figure 1). When cells are immobilized directly on the gold sensor chip, the refractive index was expected to change as a result

of drug-cell interactions on the sensing surface leading to a change in the SPR angle. The second approach considered the possibility to measure the amount of test compound that is disappearing from the surrounding liquid when the test compound interacts with or is absorbed by the cells immobilized on the roof of the flow channel.

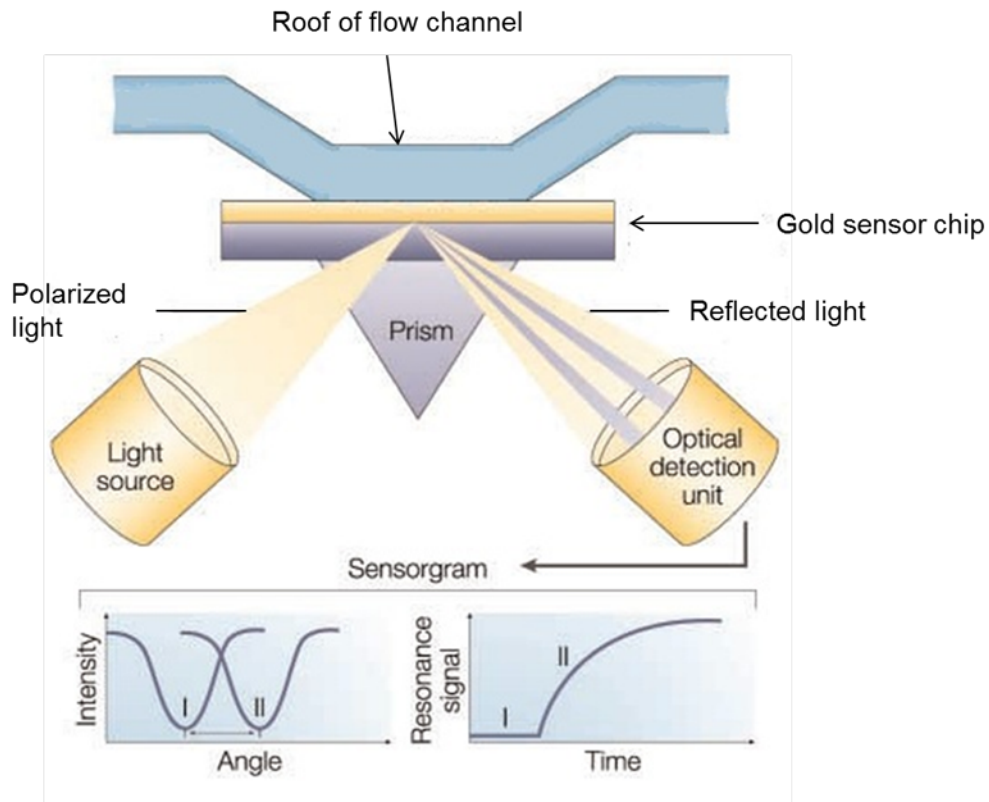


Figure 1. The principle of SPR detection using the conventional Kretschmann optical configuration. SPR detects changes in the refractive index in the immediate vicinity of the sensor surface. It appears as a sharp dip in the reflected light from the surface at an angle that is dependent on the mass of molecules on the surface (left bottom image). The SPR angle shifts when molecules bind to the surface and mass on the surface is changed. The change can be monitored by plotting the resonance signal versus time which forms sensorgram (right bottom image) (Edited from Cooper 2002).

The sensor chip and the roof of the flow channel have been made from different materials. The sensor chip is plated with gold and the roof of the flow channel is molded from poly-dimethylsiloxane (PDMS). Therefore, this study included the optimization of the immobilization conditions of cells on both of these two materials. Two cell lines, ARPE-19 and MDCKII cells were chosen for this work. The goal was first to grow cells confluent on these materials for SPR measurements. Finally, the SPR instrument was

used to probe the interaction of living cells with various test compounds, i.e. propranolol, D-mannitol, D-glucose and HSPC:Chol liposomes. For this purpose it was necessary to first optimize and choose the most convenient immobilization protocol for ARPE-19 and MDCKII cells, where after the aim was to determine if the test compounds show differences in the SPR signals upon interaction with ARPE-19 and MDCKII cells. Similar studies for ARPE-19 and MDCKII cells have not been done before.

3 MATERIALS AND METHODS

3.1 Cell culture

Human retinal pigment epithelial (ARPE-19) cells and Madin-Darby canine kidney (MDCKII) cells were used in the studies. ARPE-19 cells (passage numbers 21-35) were grown in Dulbecco's Modified Eagle Medium/Nutrient Mixture F-12 (D-MEM/F-12, Gibco) supplemented with 10 % heat-inactivated fetal bovine serum (FBS), 1 % Penicillin-Streptomycin solution and 2 mM L-Glutamine in an incubator (37 °C, 7 % CO₂). MDCKII cells (passage numbers 15-29) were cultured in Dulbecco's Modified Eagle Medium (D-MEM) (Gibco) supplemented with 10 % heat-inactivated FBS and 1 % penicillin-streptomycin solution. Cells were maintained at 37 °C in a 5 % CO₂ incubator. MDCKII cells were divided twice a week, while ARPE-19 cells were divided at one week intervals and growth medium was changed twice a week.

3.2 Immobilization of cells on the flow channel of SPR biosensor

3.2.1 Preparation of PDMS substrates

The flow channel of the SPR instrument is covered with PDMS. The aim was to immobilize the cells on the flow channel which is illustrated in Figure 2. The PDMS substrates were molded to optimize the immobilization of the cells on the material and on the flow channel. The substrates were generated by using Sylgard 184 manufactured

by Dow Corning. Sylgard 184 contains two parts: an elastomer and a curing agent that were mixed in a ratio of 10:1 by weight. The elastomer and the curing agent undergo a hydrosilylation reaction upon cross-linking. After mixing, PDMS was allowed to cure for two days at room temperature. The PDMS substrates were sterilized by immersing them in 70 % ethanol solution overnight as described by Wang et al. (2010) and Lee et al. (2004). Hereafter, the substrates were washed 2 times with DPBS (Gibco) to remove the ethanol before further modification treatment and cell culture. The optimization was first performed on a 24-well polystyrene cell plate covered with PDMS. After the conditions were defined, the cells were seeded on the molded flow channel. This flow channel was prepared by casting the PDMS mixture into the mold of the flow channel of the SPR instrument.

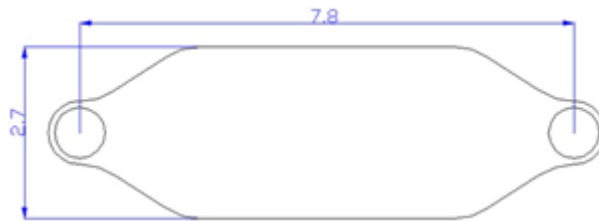


Figure 2. The dimensions (mm) of the flow channel in the SPR instrument.

3.2.2 Modification of PDMS substrates

The PDMS substrates were treated with a cell adhesion promoter in order to facilitate cell attachment on the hydrophobic PDMS surface. Several cell adhesion promoters were tested to determine the optimal component for the cell culture. PDMS substrates were rendered positively charged by treating with poly-L-lysine (PLL, Sigma-Aldrich) and with extracellular matrix (ECM) components, including fibronectin from human plasma (Sigma-Aldrich), laminin from Engelbreth-Holm-Swarm mouse tumor (BD Bioscience) or collagen type I from rat tail tendons (Trevigen).

The optimal concentration for each cell adhesion promoter was determined by screening a range of different concentrations. Table 1 shows the concentrations tested during the optimization of the cell attachment on the PDMS substrates. According to the

manufacturer's instructions each of the cell adhesion promoters were dissolved in the appropriate medium: PLL in tissue culture grade water, fibronectin in DPBS, laminin in serum-free cell culture medium and collagen I in 0,02 M acetic acid. Each PDMS surface was covered evenly with a minimal volume of the cell adhesion promoter solutions. The solutions were allowed to be in contact with the PDMS substrates for 1 h at room temperature, except for the type I collagen solution, which was kept at 37 °C. The solutions were then removed by aspiration. The substrates were rinsed twice with DPBS and allowed to dry for approximately 2 h at room temperature, where after the cells were seeded on the PDMS substrates treated with the cell adhesion promoters.

Table 1. Cell adhesion promoters and concentrations tested for modification of PDMS substrates.

Cell adhesion promoter	Tested concentration	
Poly-L-lysine	25 µg/ml	100 µg/ml
Fibronectin	15 µg/ml	30 µg/ml
Laminin	33 µg/ml	67 µg/ml
Collagen I	30 µg/ml	50 µg/ml

3.2.3 Culturing of ARPE-19 cells on PDMS substrates

ARPE-19 cells were cultured on both treated and non-treated PDMS substrates. The protocol described in section 3.2.2 was used to treat the PDMS substrates. ARPE-19 cells were seeded at a density of $1,2 \times 10^5$ cells/well (24-well plate). ARPE-19 cells were also seeded on the flow channel (Figure 2) of molded PDMS substrates treated with fibronectin (15 µg/ml). Only 15 µl of cell suspension could be used for cell seeding on the flow channel due to the small volume of the flow channel. Because of this, the cell seeding density also needed to be optimized. The tested seeding density was from 3 200 to 50 000 cells/flow channel. The cells were allowed to attach and grow on the PDMS substrates or the flow channel for one to three days in the cell culture incubator. Since PDMS is transparent, the attachment of the cells on the PDMS substrates was easily observed by using an inverted microscope (Olympus CKX31).

3.3 Culturing of cells on surface plasmon resonance gold sensor chips

SPR gold sensor chips (12 × 20 mm) were obtained from Bionavis Ltd (Tampere, Finland). The thickness of the gold layer was ~48 nm on ~2 nm thick layer of a chromium adhesion layer on a glass slide. The gold sensor chips were thoroughly cleaned before the experiments to remove all the contaminants on the gold surface and reduce any optical disturbance on the glass side. The cleaning solution consisted of 1 part of 30% ammonia hydroxide solution (Sigma) and 1 part of 30 % hydrogen peroxide (Sigma) in 5 parts Milli-Q-water. The gold sensor chips were boiled in the solution for 5 min, followed by rinsing thoroughly with Milli-Q-water and dried with nitrogen. Finally, the gold sensor chips were autoclaved before cell immobilization.

3.3.1 Modification of gold sensor chips

Prior to cell culture, the gold sensor chips were first treated with cell adhesion promoters in order to observe, if the cells would adhere better on treated gold sensor chips. The gold sensor chips were treated with 100 µg/ml PLL in tissue culture grade water (Sigma-Aldrich) or 15 µg/ml fibronectin in DPBS (Sigma-Aldrich). First, the autoclaved gold sensor chips were rinsed twice with DPBS. Then, the gold sensor chips were covered with a minimal volume of PLL or fibronectin solution and incubated for 1 h at room temperature. The cell adhesion promoter solutions were then removed by aspiration and the gold sensor chips treated with PLL were rinsed twice with DPBS. The treated gold sensor chips were then allowed to dry for 2 h at room temperature before cells were seeded.

3.3.2 Immobilization of cells on gold sensor chips

ARPE-19 and MDCKII cells were cultured on both treated and non-treated gold sensor chips. First, confluent cell monolayers in cell culture flasks were treated with 0,25 % trypsin/EDTA in DPBS, where after the cells were re-suspended in the cell culture medium. The gold sensor chip was then placed in a cell culture polystyrene petri dish with a cell growth area of 8,8 cm² and 3 ml of the cell suspension was pipetted on the

gold sensor chip. The cells were allowed to attach and grow in the incubator until they were confluent. Seeding density (from 5×10^5 to $8,8 \times 10^5$ cells/petri dish) and days post-seeding (from one to four days) were optimized to determine the best conditions for the cells to attach to the gold sensor chips. This procedure was simultaneously done on several gold sensor chips. The sensor chips were observed through a microscope to assess the cell monolayer confluence and to ensure the reproducibility of the cell culturing protocol and consequently the SPR measurements.

3.4 Viability of cells on PDMS substrates and gold sensor chips

3.4.1 Trypan blue test

The trypan blue test was performed to ensure the viability of cells cultured both on the PDMS substrates and the gold sensor chips. Cells cultured on tissue culture treated polystyrene wells were used as reference. After one or two days of culture, the medium was carefully removed and the cells were washed with DPBS before detaching with 0,25% trypsin/EDTA solution. The cells were re-suspended in the cell culture medium, then trypan blue solution (Gibco) was added in a ratio of 1:1 (v/v) in order to stain the dead cells blue. The cell concentration and cell viability was determined with a Cedex XS cell counter (Roche Diagnostics Oy).

3.4.2 MTT assay

The MTT assay was performed in order to determinate the viability of the cells cultured on the gold sensor chips. Non-treated cells grown on standard polystyrene well plate were used as a positive control (100% viability), whereas cells treated with Triton-X 2 % (Fluka) served as a negative control (0% viability). The MTT assays were performed two days post-seeding in the case of ARPE-19 cells, and three days post-seeding in the case of MDCKII cells. First, the cells were washed with DPBS, followed by addition of the MTT solution (5 mg/ml in DPBS, Sigma), and then incubating them at 37 °C for 2 h. The formazan crystals formed were dissolved by adding SDS-DMF solution (20% SDS (Bio-Rad) in DMF, Fluka) at pH 4.7 (adjusted with 80% acetic acid : 1 M HCl 1:1

by volume). Cell culture plates were then incubated overnight at 37 °C to allow complete dissolution of the formazan crystals. The amount of formazan was determined colorimetrically at a wavelength of 595 nm using a spectral scanning multimode reader Varioskan (Varioskan Flash 2.4.3. Thermo Scientific).

3.5 Flow experiments with the immobilizer

The SPR instrument used in this work has a flow channel system consisting of two separate flow channels, which are operated by the same peristaltic pump. The liquid flowing in the flow channels is in direct contact with the gold sensor chip and the height of the flow channel is 100 μm . An equipment called “the immobilizer” (Figure 3), compatible with the gold sensor chips and the slide holder of the instrument, was used to study how ARPE-19 and MDCKII cells resisted the shear stress induced by the liquid flow. The immobilizer is composed of a plain flow system without peristaltic pump thus, an external syringe pump was used (SPR Navi 200 syringe pump –module) for these studies. The height of the flow channel in the immobilizer is 300 μm . The flow experiments were performed by flowing the buffer, Hank’s Balanced Salt Solution (HBSS, Gibco) supplemented with 10 mM HEPES (Sigma-Aldrich) at pH 7.4 (adjusted with 1 M NaOH) at flow rates from 5 to 120 $\mu\text{l}/\text{min}$. The effect of the flow was observed for 15 min to 3 h at room temperature to investigate how long the cells stayed attached to the gold sensor chip under constant flow. After the cells were exposed to the flow they were observed by an optical microscope.

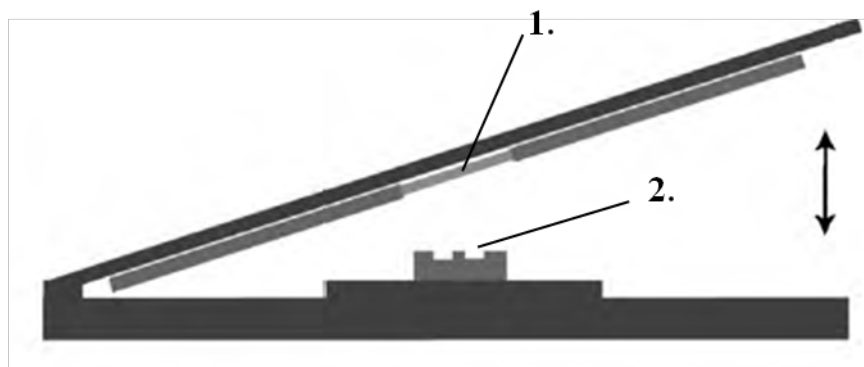


Figure 3. Schematic picture of the immobilizer without an external peristaltic pump. The numbered parts are: (1) gold sensor chip and (2) flow channel (Edited from Liang et al. 2010)

Because the height of the flow channel is not the same in the immobilizer and the SPR instrument, it was necessary to use different flow rates in the immobilizer and the SPR instrument in order to make sure that the flow conditions were comparable with each other. The shear stress on the sensor surface induced by the liquid flow is taken as a measure for the hydrodynamic conditions in the flow channel and it is dependent on the dimensions and the footprint of the flow channel (Viitala et al. 2012). The shear stress in the flow channel with the same footprint is given by the following equation:

$$S = f \times \frac{1}{h^2} \quad (1)$$

where S is shear stress, f the flow rate and h the height of the flow channel. The conversion factor for the flow speed giving the same hydrodynamic conditions in the flow channel of the immobilizer and the SPR instrument can be obtained by substituting the heights of the immobilizer (300 μm) and the flow channel in the SPR instrument (100 μm) into equation 1.

$$f_{100\mu\text{m}} \times \frac{1}{h_{100\mu\text{m}}^2} = f_{300\mu\text{m}} \times \frac{1}{h_{300\mu\text{m}}^2}$$

$$f_{100\mu\text{m}} = f_{300\mu\text{m}} \times h_{100\mu\text{m}}^2 \times \frac{1}{h_{300\mu\text{m}}^2} = f_{300\mu\text{m}} \times 100^2 \times \frac{1}{300^2} = f_{300\mu\text{m}} \times 0,111$$

The above calculation reveals that the flow rate had to be nine times higher in the immobilizer than in the SPR instrument in order to obtain comparable shear stresses in both equipments.

3.6 Test compounds in surface plasmon resonance analysis

Propranolol hydrochloride (Sigma-Aldrich), D-mannitol (Fluka), D-glucose monohydrate (Riedel-de Haen) and liposomes consisting of fully hydrogenated soy phosphatidylcholine (HSPC, Avanti Polar Lipids) and cholesterol (chol, Avanti Polar Lipids) were used as test compounds in the SPR interaction studies with living cells. Each test compound was diluted in a buffer composed of HBSS supplemented with 10 mM Hepes (Sigma) and adjusted to pH 7,4 with 1 M NaOH. HSPC:Chol liposomes with the molar ratio 2:1 were prepared using the traditional extrusion technique. The

liposomes were diluted in HBSS buffer to a HSPC concentration of 1 mM. All test solutions were sonicated before the SPR measurement to minimize the formation of air bubbles during the measurement.

3.7 Surface plasmon resonance analysis

Interaction experiments between each test compound and immobilized cells were performed using the SPR Navi 200 instrument (Bionavis Ltd, Tampere, Finland). The cells were cultured on the gold sensor chip for three to four days before analysis. Prior to the measurement, the whole flow path of the SPR instrument was filled with the running buffer HBSS. Once the cells were confluent on the gold sensor chip, the cells were washed once with the buffer and the gold sensor chip was quickly inserted into the slide holder using tweezers. Hereafter, the glass side of the sensor chip was cleaned with 70 % ethanol to remove any optical disturbances from the surface and the slide holder was then inserted in the instrument.

The SPR experiments were performed under constant flow using a syringe pump accessory (SPR Navi 200 syringe pump –module) at a flow rate of 5 $\mu\text{l}/\text{min}$ for ARPE-19 cells, and at a flow rate of 10 $\mu\text{l}/\text{min}$ for MDCKII cells. The interaction between cells and test compounds were measured by injecting the compound of interest for 6-10 min followed by a rinsing period of 6-10 min with the buffer. The samples were injected manually with a syringe to two sample loops through an injection port in a series of increasing concentrations. The sample loops were flushed with the buffer after every sample injection to avoid any carryover effect. All the experiments were performed at 20 °C by using the angular scan mode. The angular scan mode measures the change of the SPR peak minimum angular position (the SPR angle) in a selected angular scan range. In these experiments the selected angular scan range was at least 60 - 78°, which provided the full SPR angular spectra every 4th second. The full SPR angular spectra means that not only the change in the SPR peak minimum angular position but also e.g. the change in the SPR peak minimum intensity can be measured. At the end of each experiment, the SPR sensor slide was observed under an optical

microscope in order to evaluate the cell monolayer integrity after the interaction experiments.

3.8 Data handling

A widely accepted simplification for the measured SPR signal is that the change in the SPR peak minimum position (angle or wavelength) or fixed angle intensity is linearly proportional to the mass change in the evanescent field. The experiments in this work were performed using the angular scan mode, which monitors the change in the SPR angle in real-time. Briefly, the SPR instrument monitors the change of the refractive index on the surface of gold sensor chip which is reflected as a change in the SPR angle. The angular change is plotted in a sensorgram which shows the change in the SPR angle in real-time. Figure 4 illustrates the steps of a simple biomolecular interaction SPR analysis. Furthermore, the SPR instrument used in this work also provides other information than the angular change information. For example, it is also possible to observe the change in the SPR peak minimum intensity during the measurements. The SPR angle and/or the SPR peak minimum intensity is expected to change in SPR measurements with immobilized cells which is caused by changes in the reflectance properties of the cell monolayer due to morphological changes induced by exogenous stimulation.

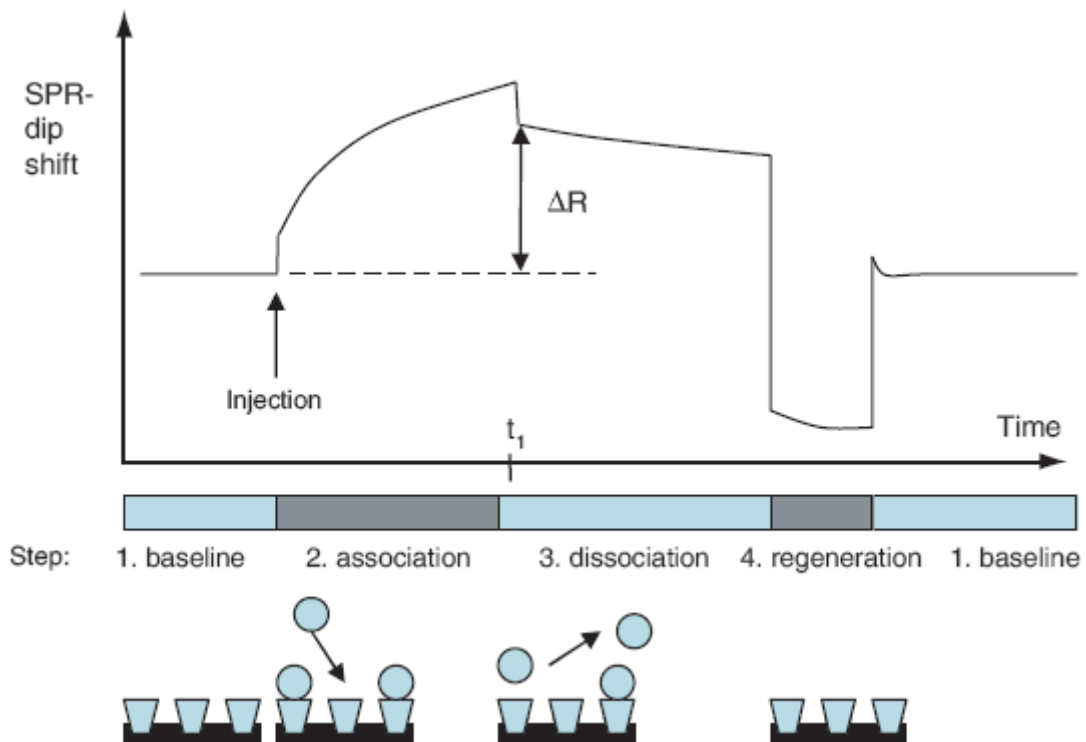


Figure 4. Sensorgram showing the steps of a simple SPR measurement where a receptor is immobilized on the gold sensor chip. 1) A buffer is contacted with the receptor through a flow channel. 2) Continuous injection of a solution of an analyte in the buffer. When the analyte binds to the receptor, then the refractive index in the near vicinity of the sensor surface increases leading to an increase in the SPR angle. 3) Injection of buffer on the gold sensor chip flushes off the non-specifically bound components. ΔR indicates the angular change caused by the bound analyte. 4) A regeneration solution is injected, which breaks the specific binding between the analyte and the receptor (Tudos and Schasfoort 2008).

4 RESULTS

4.1 Attachment and proliferation of ARPE-19 cells on PDMS substrates

ARPE-19 cells were cultured on PDMS to observe if the cells can be grown on the PDMS flow channel of the SPR instrument. In this approach the objective was to grow the cells as a confluent monolayer on the flow channel of the SPR instrument, and then probe the interaction between the cells and the test compounds in order to measure the amount of test compound that is disappearing from the surrounding liquid because of the drug-cell interaction. Since the real PMDS flow channel has a very small area where

the cells can be seeded it was first necessary to optimize the immobilization of cells on PDMS molded in 24-well plates. Figure 5 shows the microscopy images of ARPE-19 cells cultured on the PDMS substrates and in traditional polystyrene well plates. These microscopy images clearly show that the ARPE-19 cells did not adhere on non-treated PDMS substrates. The cells were floating in the cell culture medium and some of them just adhered to other cells without contacting the PDMS surface. These results indicate that PDMS with a common 10:1 elastomer to curing agent mixing ratio did not support the attachment of ARPE-19 cells.

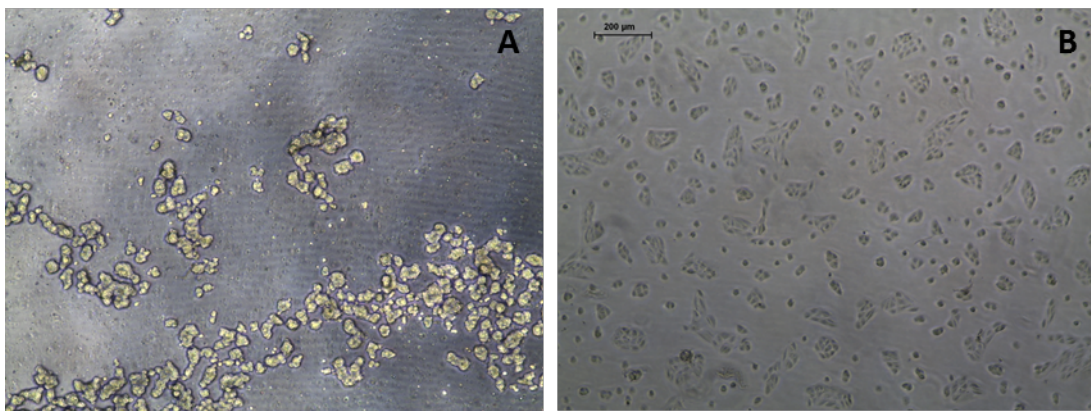


Figure 5. Light microscopy images of ARPE-19 cells cultured on A) non-treated PDMS substrate and (B) polystyrene well plate for one day. Magnification in images is 5x. Scale bar represent 200 μm .

Because ARPE-19 cells did not adhere on non-treated PDMS, the modification of the PDMS substrates was required. The PDMS substrates were modified with poly-L-lysine, fibronectin, laminin or type I collagen to promote cell adhesion and growth by physical adsorption of the cell adhesion promoter on the PDMS surface. These cell adhesion promoters were selected because they have been applied earlier for the same purpose by Wang et al. (2009). As illustrated in Figure 6, differences in the attachment and proliferation of ARPE-19 cells could be detected depending on the cell adhesion promoter used. From all the tested materials PDMS treated with fibronectin was found to support the attachment and proliferation of ARPE-19 cells to a similar extent as the polystyrene well plate, which was used as a control. In this case, cell confluence level was about 100% after two days of culture and the shape of the ARPE-19 cells was similar to the cells cultured on polystyrene. It was also found that 15 $\mu\text{g/ml}$ fibronectin

enhanced the attachment of ARPE-19 cells to the same extent as the higher concentration of fibronectin (30 $\mu\text{g/ml}$).

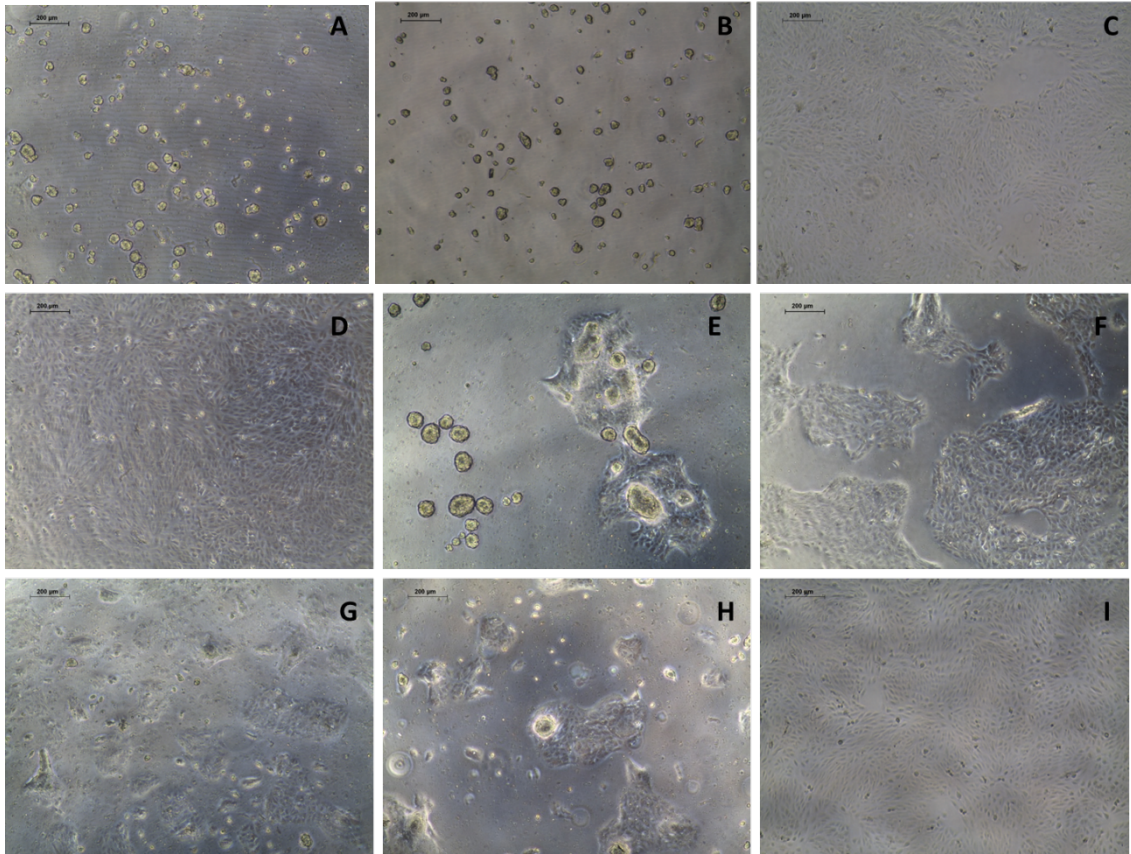


Figure 6. Growth of ARPE-19 cells after two days seeding on the PDMS substrates treated with different cell adhesion promoters: A) 25 and B) 100 $\mu\text{g/ml}$ poly-L-lysine, C) 15 and D) 30 $\mu\text{g/ml}$ fibronectin, E) 30 and F) 50 $\mu\text{g/ml}$ type I collagen and G) 33 and H) 67 $\mu\text{g/ml}$ laminin. The cells growing on a traditional polystyrene well plate were used as a control (I). Magnification in images is 5x. Scale bars represent 200 μm .

In addition to the microscopic observations, the proliferation of ARPE-19 cells was determined with trypan blue test after one and three days of culture. The number of viable cells cultured on the treated PDMS substrates is illustrated in Figure 7. After three days, the number of living cells had increased for all ECM proteins, except for the type I collagen (30 $\mu\text{g/ml}$). Laminin enhanced the initial attachment of the cells on PDMS, but the proliferation was slower than on polystyrene. The modification with fibronectin had a significant effect on the number of living cells growing on PDMS. In this case, the proliferation of ARPE-19 cells was of the same as on polystyrene.

Moreover, the trypan blue test showed a cell viability of 98,7% (n=2) determined for the cells cultured on 15 μ g/ml fibronectin-treated PDMS for three days, which was basically the same as the cell viability of 98,6 % (n=2) on polystyrene. The proliferation of the cells on poly-L-lysine-treated PDMS was not determined because it did not promote the adhesion of ARPE-19 cells based on the microscopic observations (Figure 6A-B).

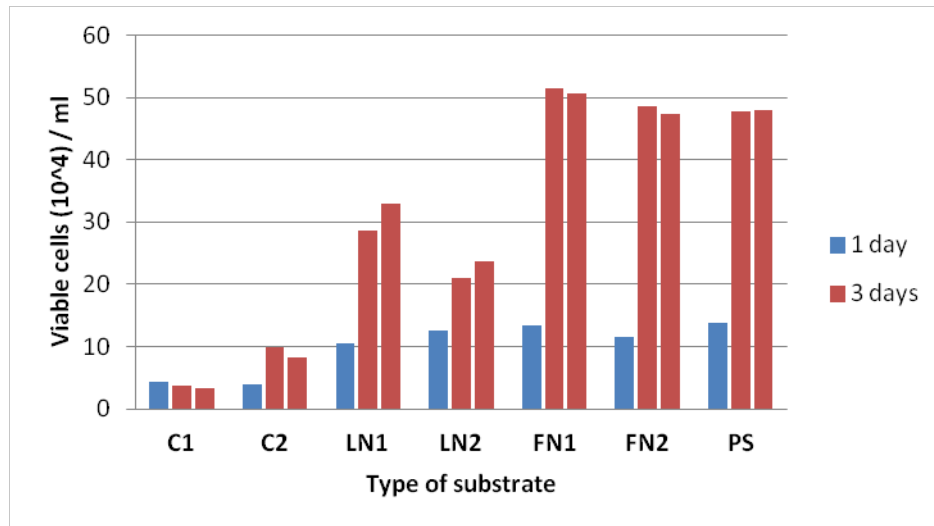


Figure 7. Number of viable ARPE-19 cells cultured on the treated PDMS substrates modified with different ECM proteins: 30 (C1) and 50 μ g/ml type I collagen (C2), 33 (LN1) and 67 μ g/ml laminin (LN2), and 15 (FN1) and 30 μ g/ml fibronectin (FN2). The cells growing on polystyrene well plate were used as a control. The cells were counted one (n=1) and three days (n=2) post-seeding.

These results show that ARPE-19 cells can be grown confluent and viable on the fibronectin-treated PDMS substrates. For this reason, fibronectin (15 μ g/ml) was the cell adhesion promoter selected to treat the PDMS molded flow channel. However, the seeding of the cells on the fibronectin-treated PDMS molded flow channel was not straightforward because of the small volume of the flow channel. Therefore, only 15 μ l of cell suspension could be used for the cell seeding on the PDMS molded flow channel. Moreover, the visualization of the immobilized ARPE-19 cells on the PDMS molded flow channel was rather challenging as illustrated in Figure 8. Different cell seeding densities were also tested because it was anticipated that successful SPR measurement would require confluent cell monolayers grown on the flow channel. However, it was not possible to select the optimal seeding density based on light

microscope visualization, because it was not possible to easily separate the cells from the surface of the PDMS molded flow channel by an optical microscope. Based on these results it was decided that no further attempts to grow cells on the PDMS flow channel in the SPR instrument would be made, and that it would be more important to concentrate on the second approach where cells would be directly immobilized on the gold sensor chips.

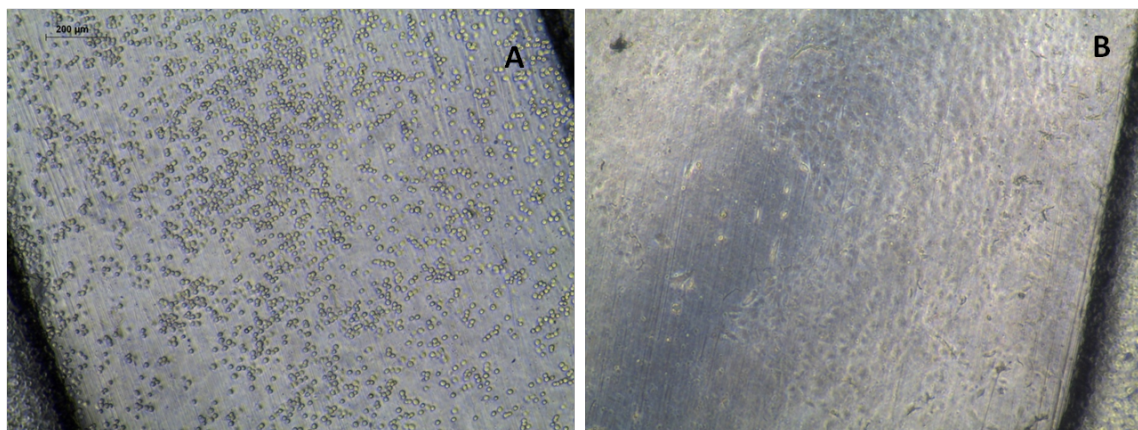


Figure 8. ARPE-19 cells cultured on the flow channel molded from PDMS: A) 1 hour and B) 48 hours after seeding. Magnification in images is 5x.

4.2 Growing and viability of the cells on gold sensor chip

The immobilization of ARPE-19 and MDCKII cells on the gold sensor chips was optimized for the second approach of this work, where the objective was to culture the cells directly on the gold sensor chip. In this approach, the refractive index was expected to change as a result of drug-cell interactions on the sensing surface leading to a change in the SPR angle. In order to ensure the repeatability of the SPR measurements and to avoid unspecific adsorption of the test compounds on the bare gold surface, it was necessary to grow confluent cell monolayers in the middle of the gold sensor chip, where the change in the refractive index is measured. First, the growing of the cells was observed through a microscope to study if the cells grow confluent on the non-treated gold sensor chip, and if treatment of the gold sensor chip was needed in order to attach the cells to the surface. The cell spreading is generally assumed to give only an

indication of cell adhesion. Therefore, also the viability of the cells on the gold sensor chips was studied using both trypan blue test and the MTT assay.

4.2.1 ARPE-19 cells

ARPE-19 cells were cultured on non-treated gold sensor chips and gold sensor chips treated with poly-L-lysine (100 $\mu\text{g/ml}$) or with fibronectin (15 $\mu\text{g/ml}$). PLL was chosen because it is widely used to promote cellular adhesion to a surface by providing a polycationic layer on the substrate interacting with the polyanionic cell surfaces (Yavin and Yavin 1974). Moreover, PLL has earlier been utilized in SPR studies with cells by Chabot et al. (2009) in order to attach cells to a gold sensor chip. Fibronectin was selected because it is an ECM glycoprotein, which modulates the cell attachment by its arginine-glycine-aspartic acid cell adhesion peptides that adhere to the surface and interact with the cells (Rezania and Healy 1999).

The cell adhesion and growth of ARPE-19 cells were followed during three days. Figure 9 shows microscopy images of cells that have adhered on the surface of the gold sensor chips after three days of culture. The attachment and proliferation of ARPE-19 cells on non-treated and fibronectin-treated gold sensor chips was similar as on polystyrene. In these three different cases, cells were growing confluent on the surfaces but the treatment with PLL appeared to suppress the proliferation of the cells. Thus, the microscopic images indicated that the treatment of the gold sensor chips with an adhesion promoter was not needed to successfully immobilize a confluent ARPE-19 cell monolayer on the gold sensor chips.

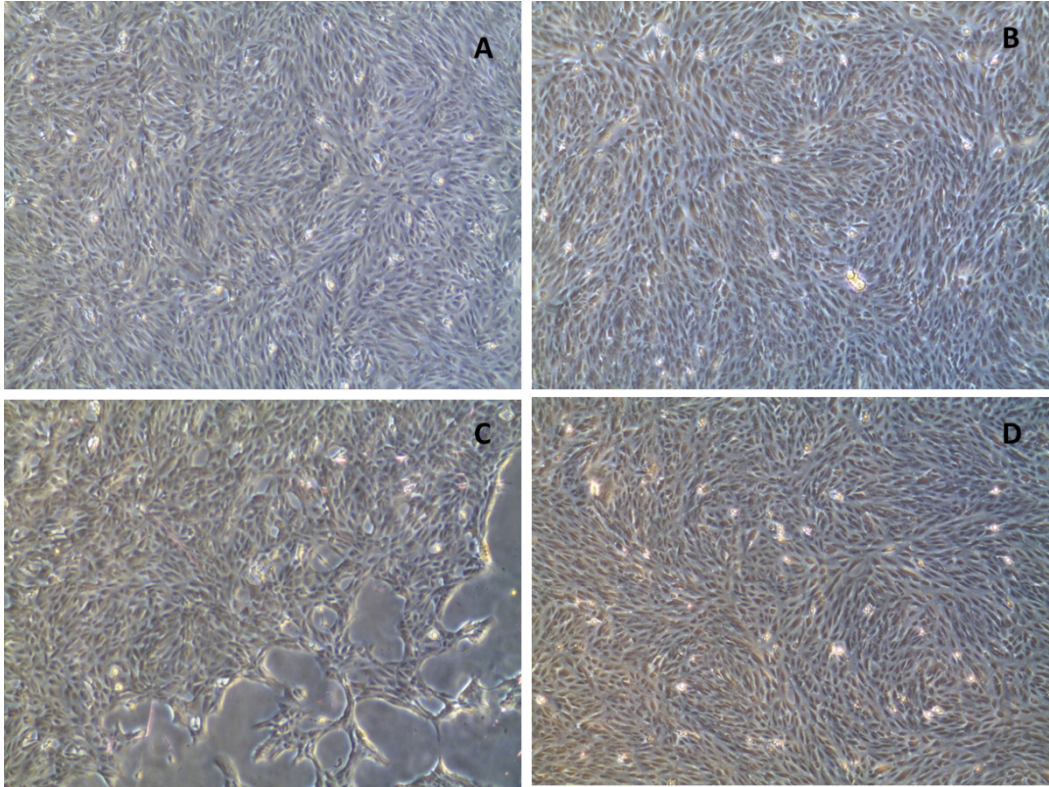


Figure 9. Light microscopy images of ARPE-19 cells cultured for three days on A) gold sensor chip, B) gold sensor chip treated with fibronectin and C) with poly-L-lysine and D) polystyrene well plate. Magnification in images is 5x.

The trypan blue and the MTT assay were performed to detect the viability of ARPE-19 cells cultured on non-treated and fibronectin-treated gold sensor chips. According to the test results, the culturing on the gold sensor chips had no significant inhibitor effect on the cell viability after one and two days of culture (Figure 10). The trypan blue test showed that the viability of the cells on the gold sensor chip was similar as on polystyrene, which was used as a control (Figure 10A). Furthermore, the MTT assay confirmed that the culturing of ARPE-19 cells on the gold sensor chip did not decrease the viability of the cells after two days of culture (Figure 10B). The percentage of viable cells cultured on non-treated gold sensor chip was $111,3 \pm 10,3\%$ and $105,6 \pm 11,1\%$ on the fibronectin-treated gold sensor chips.

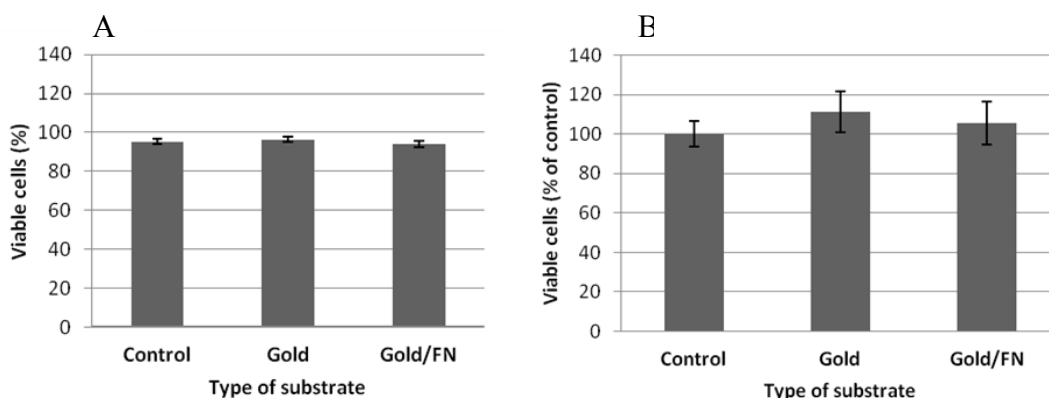


Figure 10. Viability of ARPE-19 cells cultured on non-treated gold sensor chips, gold sensor chips treated with fibronectin (15 $\mu\text{g/ml}$) and traditional polystyrene well plate (control) assessed by A) trypan blue and B) MTT assay. The trypan blue test was performed one day and the MTT assay three days post-seeding. Reported values and standard errors are average of three parallel experiments.

4.2.2 MDCKII cells

MDCKII cells were cultured both on non-treated and fibronectin-treated (15 $\mu\text{g/ml}$) gold sensor chips. The growth of MDCKII cells on the gold sensor chips was followed during three days. Figure 11 shows microscopy images of cells that have adhered on the surface of the gold sensor chips after three days of culture. According to the microscopic observation it was clear that MDCKII cells also adhered on the surface of the non-treated gold sensor chips. The growth and attachment of MDCKII cells on the gold sensor chips were similar as on polystyrene. The microscopy images thus revealed that pre-treatment of the gold sensor chips with an adhesion promoter was not necessary to successfully immobilize a confluent MDCKII cell monolayer on the gold sensor chips.

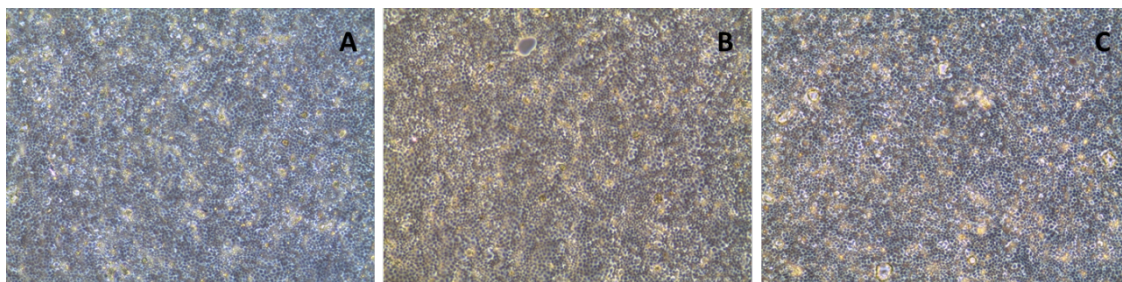


Figure 11. Light microscope images of MDCKII cells cultured for three days on A) a non-treated gold sensor chip, B) gold sensor chip treated with 15 $\mu\text{g/ml}$ fibronectin and C) polystyrene well plate. Magnification in images is 5x.

However, the microscopy images revealed that MDCKII cells formed clusters when they were cultured fully confluent on the smooth non treated gold sensor chip surface. For this reason, the cell density needed to be carefully controlled. The seeding density was optimized so that the cells grew confluent with the lowest possible amount of the seeded cells (Figure 12). Based on the microscopic observations of different cell seeding densities it was found that the optimum seeding density that produced a cluster free confluent cell monolayer was 7×10^4 cells/cm² and this was selected for the further experiments.

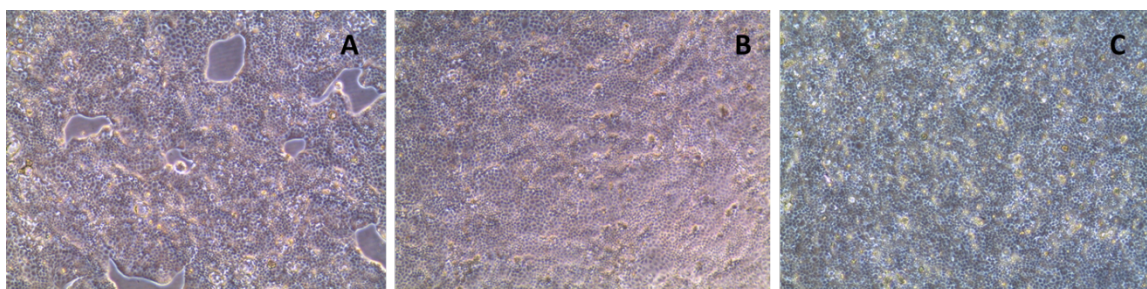


Figure 12. Light microscope images of MDCKII cells with different seeding density grown on non-treated gold sensor chips for three days. Cell seeding density: A) 5×10^4 cells/cm², B) 7×10^4 cells/cm² and C) 1×10^5 cells/cm².

According to the results of the trypan blue and the MTT assays, culturing the cells on a non-treated gold sensor chip surface did slightly decrease the viability of the MDCKII cells after one and three days of culture (Figure 13). According to the trypan blue assay, the percentage of viable cells seeded on non-treated gold sensor chip surfaces were $90,4 \pm 3,5\%$ and on polystyrene wells $92,6 \pm 2,2\%$. In the case of the MTT assay the mean

cell viability value obtained for cells cultured on non-treated gold sensor chips was $81,5\pm 8,9\%$, when the absorbance values obtained for cells cultured on polystyrene were accepted as $100\pm 8,2\%$.

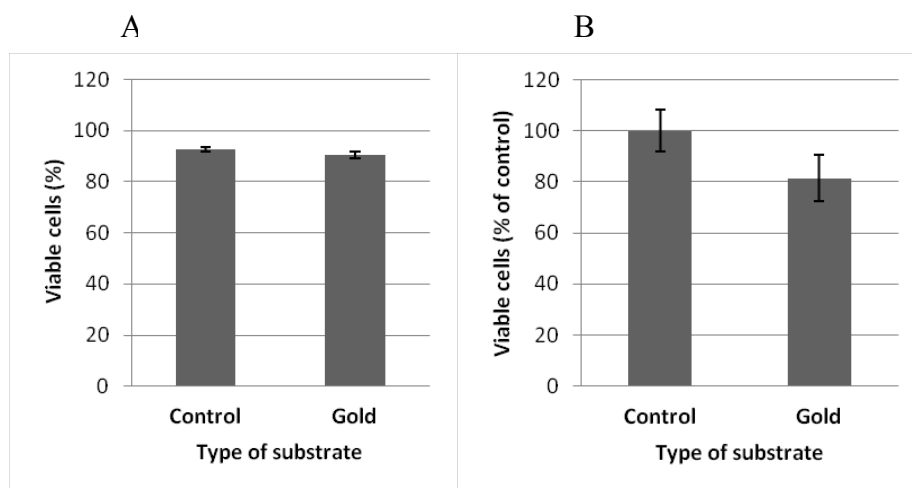


Figure 13. Viability of MDCKII cells cultured on gold sensor chips: A) Trypan blue test and B) MTT assay. MDCKII cells cultured in polystyrene well plates were used as a control. The trypan blue test was performed one day and the MTT assay three days post-seeding. Reported values and standard errors are average of six parallel experiments.

MDCKII cells were cultured only on the gold sensor chips and not on the PDMS substrates because it was difficult to visualize the cells on PDMS as shown in the case of ARPE-19 cells (Figure 8). Therefore, it was decided to perform all the drug-cell interaction measurements with SPR using the approach where the cells are immobilized directly on the gold sensor chip. This approach was chosen because both ARPE-19 and MDCKII cell lines were growing confluent and viable on non-treated gold sensor chips. Furthermore, the seeding process was significantly more straightforward than the immobilization of the cells on the flow channel of the SPR instrument.

4.3 Flow experiments

As illustrated in Figure 14, the examination of the gold sensor chip under an optical microscope at the end of the first SPR measurement with ARPE-19 cells revealed that the cells had detached from the surface during the measurement. For this reason, flow experiments with the immobilizer were performed before actual SPR measurements. The aim was to study the resistance of ARPE-19 and MDCKII cells immobilized on the gold sensor chips to the surface shear force created by the flow of the running buffer in the flow channel of the SPR instrument. The immobilizer is a plain accessory which mimics the flow conditions in the SPR instrument. The objective was to define the flow rate of the buffer that can be applied in the SPR measurements so that the cells remain attached as a confluent cell monolayer on the gold sensor chip during the measurement.

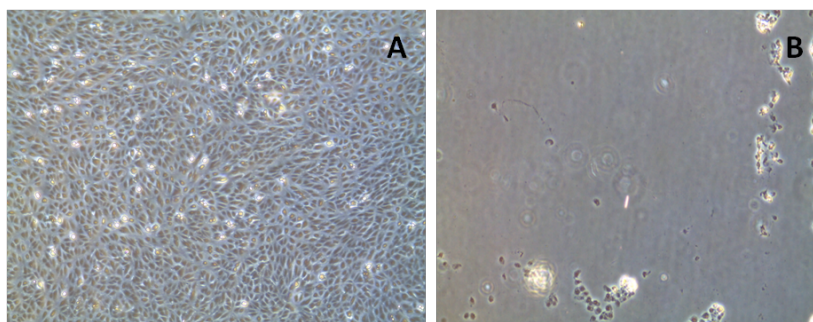


Figure 14. Light microscope images of ARPE-19 cells on a non-treated gold sensor chip A) before and B) after the SPR measurement with a flow rate of 20 $\mu\text{l}/\text{min}$ of buffer at 20 $^{\circ}\text{C}$. The cells were seeded one day before the measurement. In Figure B it can be seen how the cells have detached from the gold sensor chip. Magnification in images is 5x.

According to the results, the critical parameters identified to affect the attachment of the cells on the gold sensor chip during the SPR measurements were: cell line, cell density, days post-seeding and flow rate. The flow experiments indicated that ARPE-19 cells needed to be cultured at least two days before the SPR measurements were performed in order to attach the cells more strongly on the gold sensor chip surface. The examination under the microscope revealed that the treatment of the gold sensor chips with cell adhesion promoters was not needed, because ARPE-19 cells were attached even more confluent on a non-treated gold sensor chip compared to a fibronectin-treated gold

sensor chip after 3 hours of buffer flow at a flow rate of 5 $\mu\text{l}/\text{ml}$ (Figure 15). As the ARPE-19 cells were detaching from the gold sensor chip at higher flow rates a flow rate of 5 $\mu\text{l}/\text{ml}$ was decided to be used in the SPR measurements with ARPE-19 cells.

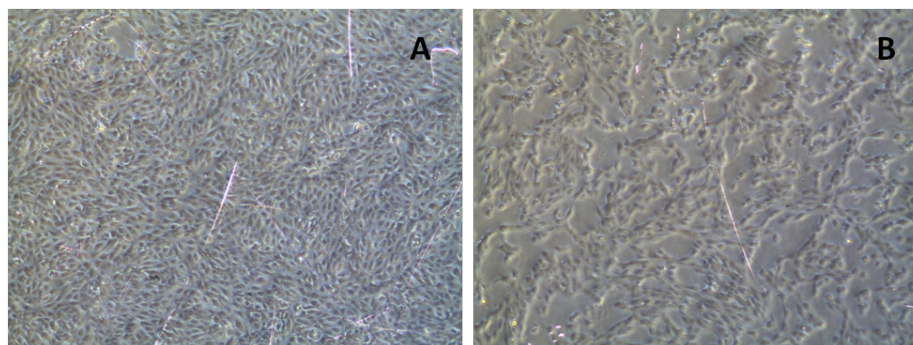


Figure 15. Light microscope images of ARPE-19 cells on A) a non-treated and B) fibronectin-treated (15 $\mu\text{g}/\text{ml}$) gold sensor chip after exposed to a buffer flow rate of 5 $\mu\text{l}/\text{min}$ for three hours in the immobilizer. The cells were seeded two days before measurement. Magnification in images is 5x.

MDCKII cells were perfused with a buffer at various flow rates ranging from 5 to 120 $\mu\text{l}/\text{min}$. These flow experiments revealed that MDCKII cells can resist the flow-induced shear stress much better than ARPE-19 cells (Figure 16). Based on these results and as described by Robelek and Weger (2010), the flow rate of 10 $\mu\text{l}/\text{min}$ was chosen for the SPR measurements with MDCKII cells. However, the examination under the microscope showed that MDCKII cells were attached as a confluent monolayer on a non-treated gold sensor chip even after being exposed to a flow rate of 120 $\mu\text{l}/\text{min}$ for approximately two hours. This may be valuable information for future studies with MDCKII cells in SPR based cell assays. The flow experiments clearly demonstrate that there is no need for pre-treatment of the gold sensor chips with cell adhesion promoters before seeding the MDCKII cells on the gold sensor chip for SPR studies with varying flow rates.


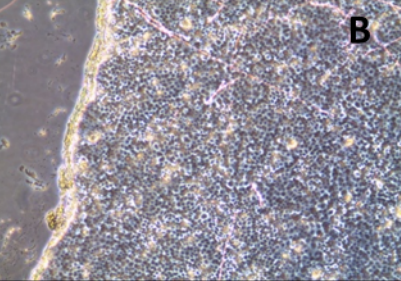
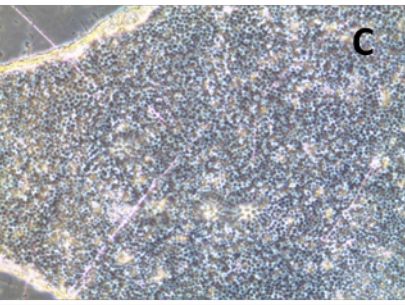
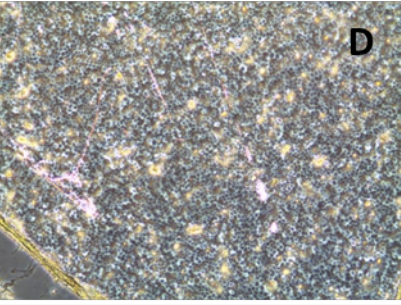
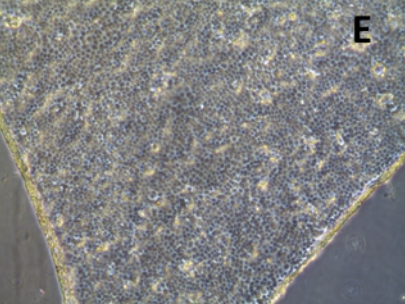
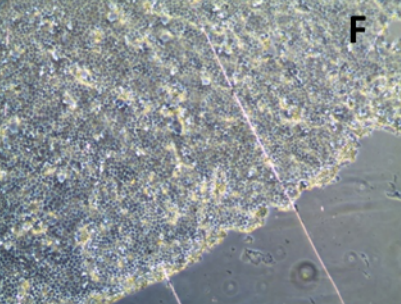
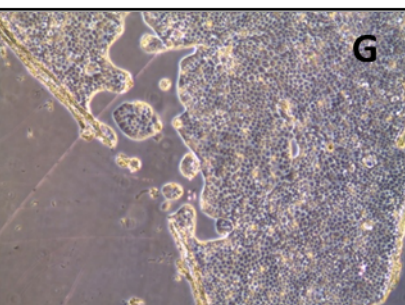
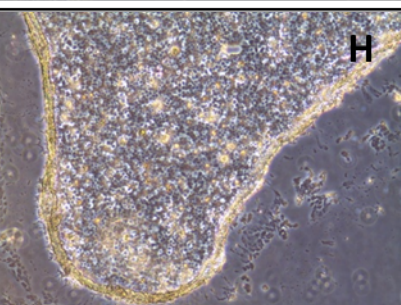
Flow rate in the SPR instrument	After flow experiment	
A Q = 5 $\mu\text{l}/\text{min}$ t = 3 h c = 96 h B Q = 10 $\mu\text{l}/\text{min}$ t = 2 h c = 72 h		
C Q = 20 $\mu\text{l}/\text{min}$ t = 30 min c = 72 h D Q = 30 $\mu\text{l}/\text{min}$ t = 3 h c = 48 h		
E Q = 40 $\mu\text{l}/\text{min}$ t = 30 min c = 96 h F Q = 50 $\mu\text{l}/\text{min}$ t = 15 min c = 96 h		
G Q = 60 $\mu\text{l}/\text{min}$ t = 15 min c = 96 h H Q = 120 $\mu\text{l}/\text{min}$ t = 1 h 45 min c = 96 h		

Figure 16. Light microscope images of MDCKII cells immobilized on the non-treated gold sensor chips after the flow experiments with the immobilizer. The parameters shown are: flow rate of buffer (Q), time in flow (t) and hours post-seeding (c). The influence of the buffer flow on the attachment of the cells on the gold sensor chip was tested with the flow rates from 5 $\mu\text{l}/\text{min}$ to 120 $\mu\text{l}/\text{min}$ for 15 min to 3 h. The flow rate shown is equivalent to that in the SPR instrument. Magnification in images is 5x.

4.4 Drug-cell interaction analysis with surface plasmon resonance

The successful immobilization of the cells as a confluent monolayer on the gold sensor chips was verified through microscopic observations before every SPR measurement. The SPR measurements were performed by using the angular scan mode which measures the SPR peak minimum angular position (the SPR angle) as a function of time. The first SPR measurement was performed by exposing ARPE-19 cells to a pure buffer at a flow rate of 5 $\mu\text{l}/\text{min}$ for two hours. During the exposure to the pure buffer, a significant decrease in the SPR angle was observed (not shown). This decrease of the SPR angle indicated that ARPE-19 cells were detaching from the gold sensor chip in the buffer flow. Indeed, after the measurement, the gold sensor chip was visualized with a microscope and the cells had detached. Attempts to overcome the problems with this cell line in the SPR measurements were tried by changing the buffer, and further trying to optimize the cell immobilization protocol on the gold sensor chip. At first, the DPBS buffer was replaced by HBSS (10 mM HEPES, pH 7,4). Secondly, the cell seeding density was changed from $5,3 \times 10^4$ to $8,7 \times 10^4$ cells/cm². Finally, the cell culturing time on the gold sensor chip was changed to three to four days instead of one day. Even, when the SPR measurement was performed with these optimized conditions, ARPE-19 cells still detached from the surface. For this reason, the SPR measurements were continued only with MDCKII cells.

MDCKII cells were exposed to the test compounds at a flow rate of 10 $\mu\text{l}/\text{min}$. Figure 18A shows a typical sensorgram of the SPR angle during an experiment when a confluent MDCKII cell monolayer was exposed to an increasing concentrations of propranolol, i.e. 2,5; 25, 50 and 250 μM . The SPR angle was displaced to lower angles during the exposure, and when the cells were only rinsed with the pure buffer after the propranolol exposure the SPR angle was displaced to higher angles compared to the baseline. An increase in the SPR angle indicates that a certain fraction of propranolol remains in the cell monolayer after the exposure. The increase in the SPR angle was clearly concentration dependent. Surprisingly, when the cells were exposed to the highest concentration of propranolol the SPR angle shift was positive, which suggests that morphological changes occurred in the immobilized cells during the exposure

(Figure 18B). As illustrated in Figure 18C, no significant change in the SPR angle was observed when propranolol was interacting with a non-treated gold sensor chip without cells. This result confirms that the change in the SPR angle measured during the interaction of propranolol with the immobilized MDCKII cells actually reflects real drug-cell interactions and not drug-gold interactions.

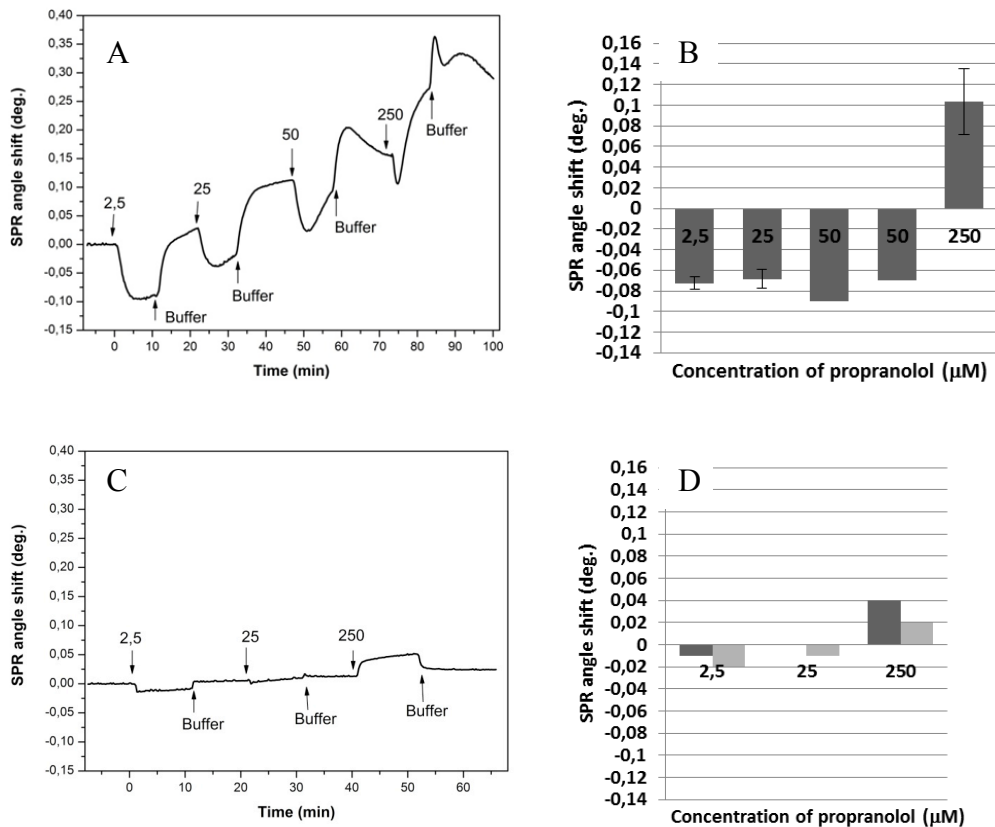


Figure 18. A) Measured changes in the SPR angle as a function of time when a MDCKII cell monolayer was exposed to propranolol (μM) for 10 min followed by rinsing with a pure buffer. Down arrows represent the time of sample injections, and up arrows the time of the injection of a pure buffer. B) Maximum measured change in the SPR angle when MDCKII cells were exposed to 2,5 (n=4); 25 (n=6), 50 (n=2) and 250 μM (n=6) propranolol. The mean and standard errors of individual measurements are shown. C) Measured changes in the SPR angle as a function of time when propranolol was interacting with a non-treated gold sensor chip without cells. D) Maximum measured change in the SPR angle when the non-treated gold sensor chip without cells was exposed to propranolol (n=2).

Furthermore, when studying the measured full SPR angle spectra during the exposure of a MDCKII cell monolayer to propranolol there was a clear change in the SPR peak minimum intensity as illustrated in Figure 19. Exposing the cells to propranolol decreased the SPR peak minimum intensity from 0,0705 to 0,0689. After the exposure, when the immobilized cells were rinsed with pure buffer, the intensity was shifted to a higher intensity (0,0791). In biomolecular assays, an increase in the SPR peak minimum intensity indicates that the sample adsorbs or scatters the light used for SPR detection. Moreover, the SPR peak minimum intensity did not shift when the measurement was done on the non-treated gold sensor chip without the cells (data not shown). Therefore, these results strongly suggest that the observed change in the SPR peak minimum intensity during propranolol interaction causes intracellular changes in the immobilized cells.

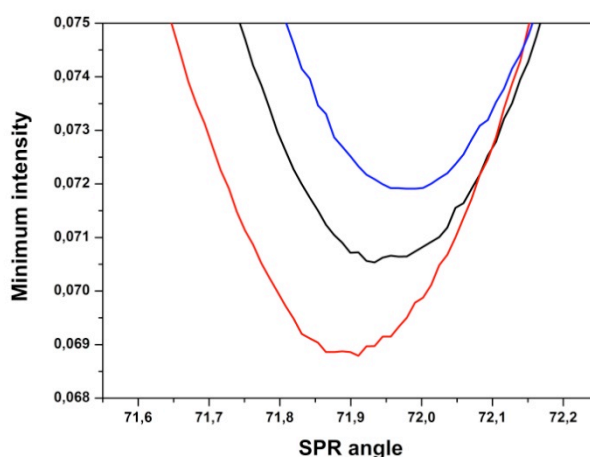


Figure 19. Focused part of full SPR angular spectra illustrating the change in the SPR peak minimum intensity of the SPR curve in the presence of MDCKII cells in a buffer flow before the exposure (black), during the exposure to 2,5 μM propranolol (red) and after the exposure in a buffer flow (blue).

In addition to propranolol, MDCKII cells were also exposed to an increasing concentration of D-mannitol. Figure 20A shows that the exposure of the cells to 0,0025; 0,025; 0,25; 2,5; 25 and 250 μM D-mannitol always caused a decrease in the SPR angle. This result indicates that even though D-mannitol diffuses poorly into the cells, some changes in the cell monolayer occurred during D-mannitol exposure. Figure 20B

illustrates the effect of D-mannitol injections on the SPR angle shift showing that the SPR angle shift was almost constant at every tested concentration, and no concentration dependency was observed. When the MDCKII cell monolayer was exposed to the pure buffer after each injection of D-mannitol, the SPR angle always returned to the baseline level. This result suggests that D-mannitol did not diffused into the immobilized cells or it was almost completely removed from the cell monolayer after the exposure regardless of the concentration used. Figure 20C and 20D also show that no significant change in the SPR angle was measured when D-mannitol was interacting with a non-treated gold sensor chip without cells.

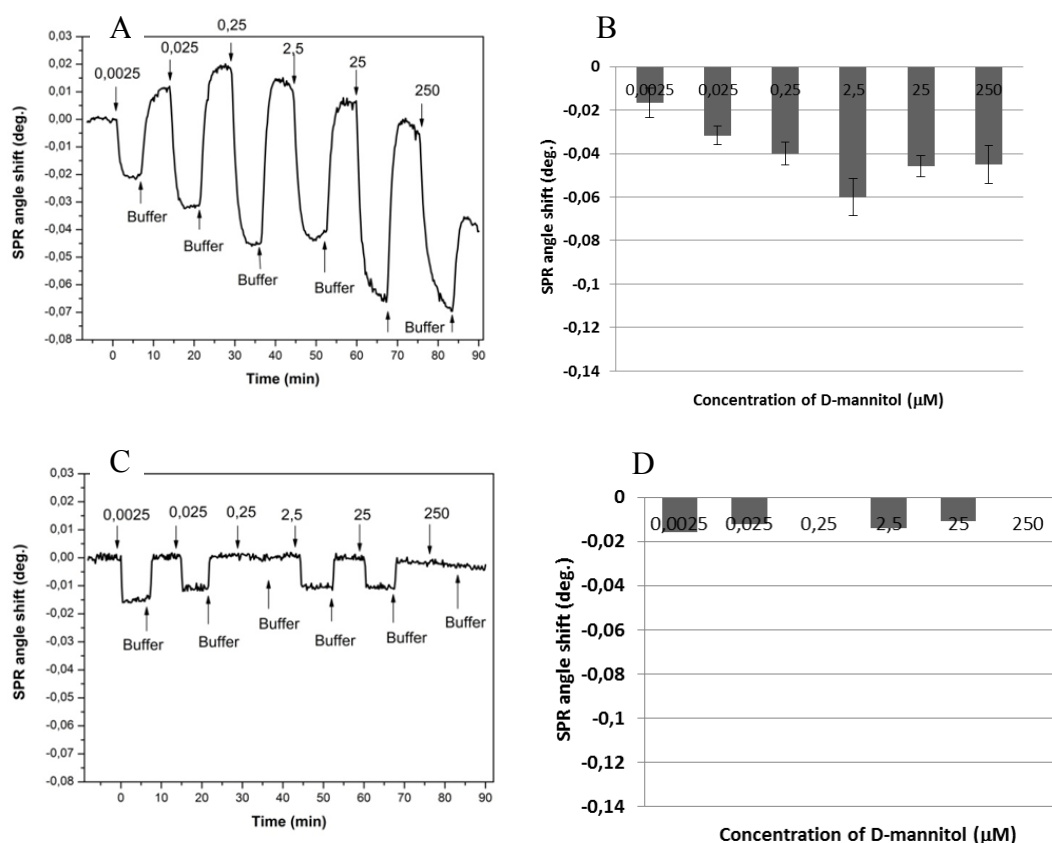
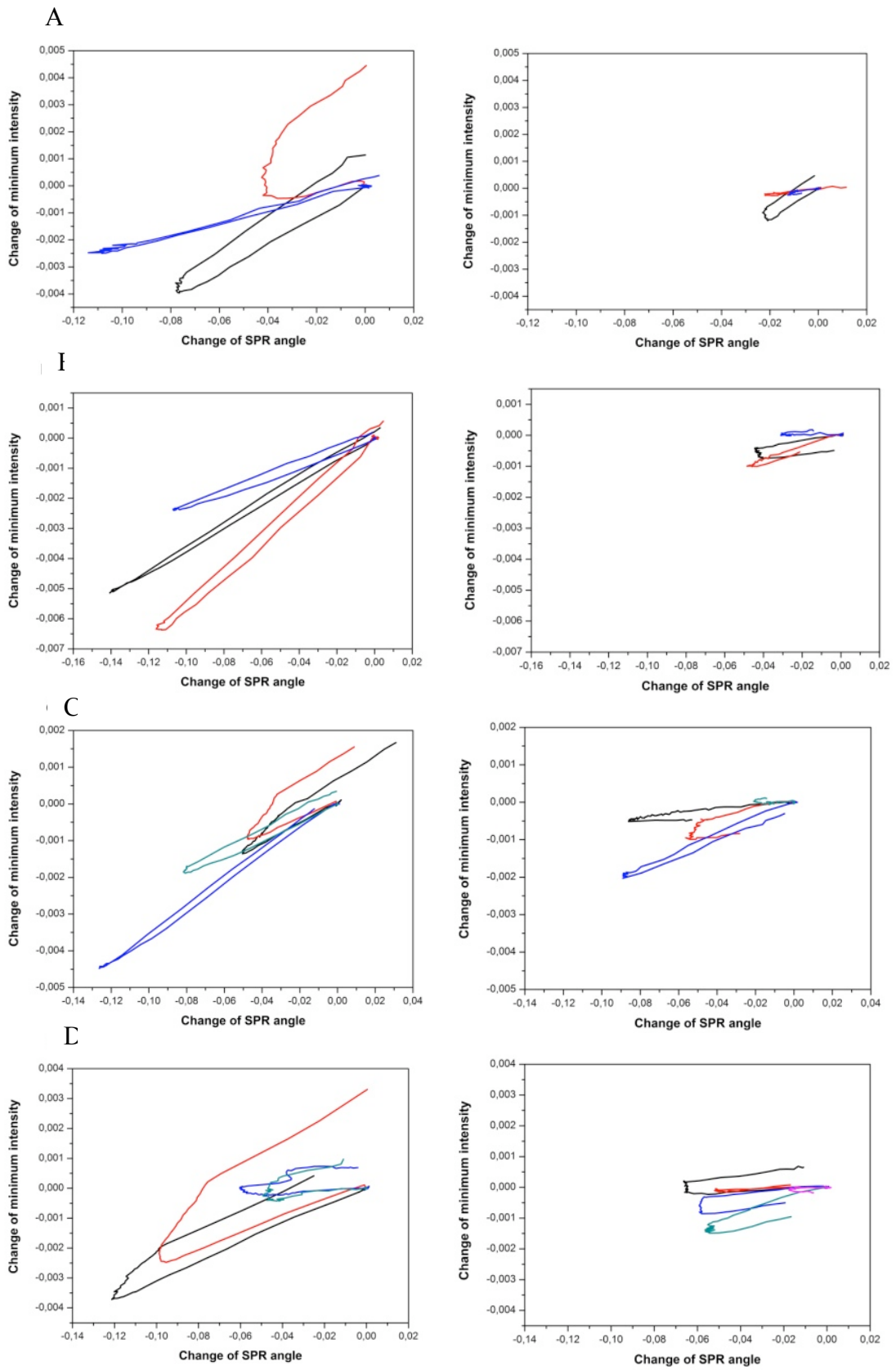


Figure 20. A) Measured changes in the SPR angle as a function of time when a MDCKII cell monolayer was exposed to D-mannitol (μM) for 7 min. Down arrows represent the time of sample injections, and up arrows the time of the injection of a pure buffer. B) Maximum measured change in the SPR angle when MDCKII cells were exposed to 0,0025 (n=3); 0,025 (n=6); 0,25 (n=6); 2,5 (n=8); 25 (n=6) and 250 μM (n=4) D-mannitol. The mean and standard errors of individual measurements are represented. C) Measured changes in the SPR angle as a function of time when D-mannitol was interacting with a non-treated gold sensor chip without cells. D) Maximum measured change in the SPR angle when a non-treated gold sensor chip without cells was exposed to D-mannitol (n=1).

Figure 21 illustrates a series of plots of the change in the SPR angle versus the change in the SPR peak minimum intensity from at least three repetitions and several concentrations when the MDCKII cell monolayer was exposed to propranolol or D-mannitol. The plots illustrate that when the cell monolayer was exposed to increasing concentrations of D-mannitol, the SPR peak minimum intensity did not change or decreased only slightly (which is seen as a horizontal appearance in the plots). In the case of propranolol, the exposure induced a significantly higher decrease in the SPR peak minimum intensity and in the SPR angle at every concentration compared to D-mannitol. This is visualized as a more vertical appearance in the plots. Moreover, the SPR peak intensity was shifted to a higher value after the exposure of propranolol when the MDCKII cells were flushed with pure buffer. This effect was not observed in the case of D-mannitol. These results clearly indicate that propranolol and D-mannitol interact differently with the MDCKII cell monolayer immobilized on the non-treated gold sensor chip. Generally, it is known that propranolol diffuses effectively by the transcellular pathway into cells whereas D-mannitol uses the paracellular pathway (Salama et al. 2003; Artursson 1990). This difference in the interaction between the test compound and the cell monolayer is observed not only in the SPR angle, but also in the SPR peak minimum intensity. The results propose that instead of analyzing only the change in the SPR angle during drug-cell interaction measurements it would be more reasonable to analyze both the SPR angle and SPR peak minimum intensity, and consequently plot them against each other in order to better understand and differentiate between the interactions between different drugs and cells.



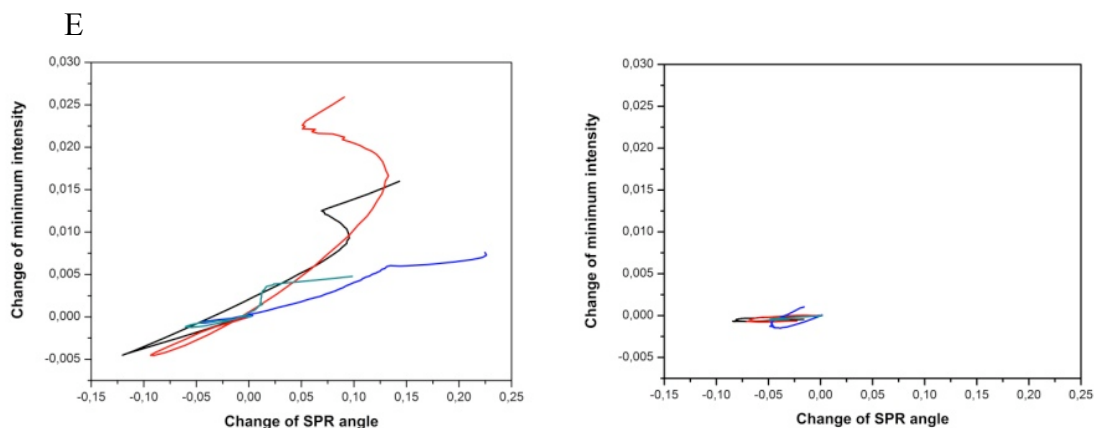


Figure 21. Change in the SPR peak minimum intensity as a function of the change in the SPR angle, when MDCKII cells were exposed to propranolol (left) and D-mannitol (right). Individual SPR measurements as concentration series: A) 0,0025; B) 0,25; C) 2,5; D) 25 and E) 250 μ M which was followed by the dissociation in pure buffer. Different colors indicate independent experiments.

The immobilized MDCKII cells were finally also exposed to several concentrations of D-glucose and HSPC:Chol liposomes. As illustrated in Figure 22, the exposure decreased the SPR angle in both cases, except for the highest concentration of D-glucose, where the angle increased, but only slightly when compared to propranolol (Figure 18B). The negative change in the SPR angle indicates that both of these test compounds also interacted with the MDCKII cell monolayer. After exposing cells to D-glucose followed by exposure to pure buffer, the SPR angle shifted to higher angles than the baseline. The SPR angle shift for glucose was in the same order of magnitude as in the case of propranolol. This increase in the SPR angle indicated that the transport of D-glucose into the cells was actually detected by SPR. On the contrary the exposure of the cells to liposomes produced a decrease in the baseline suggesting that liposomes were not taken up by the cells within the time frame of the experiments.

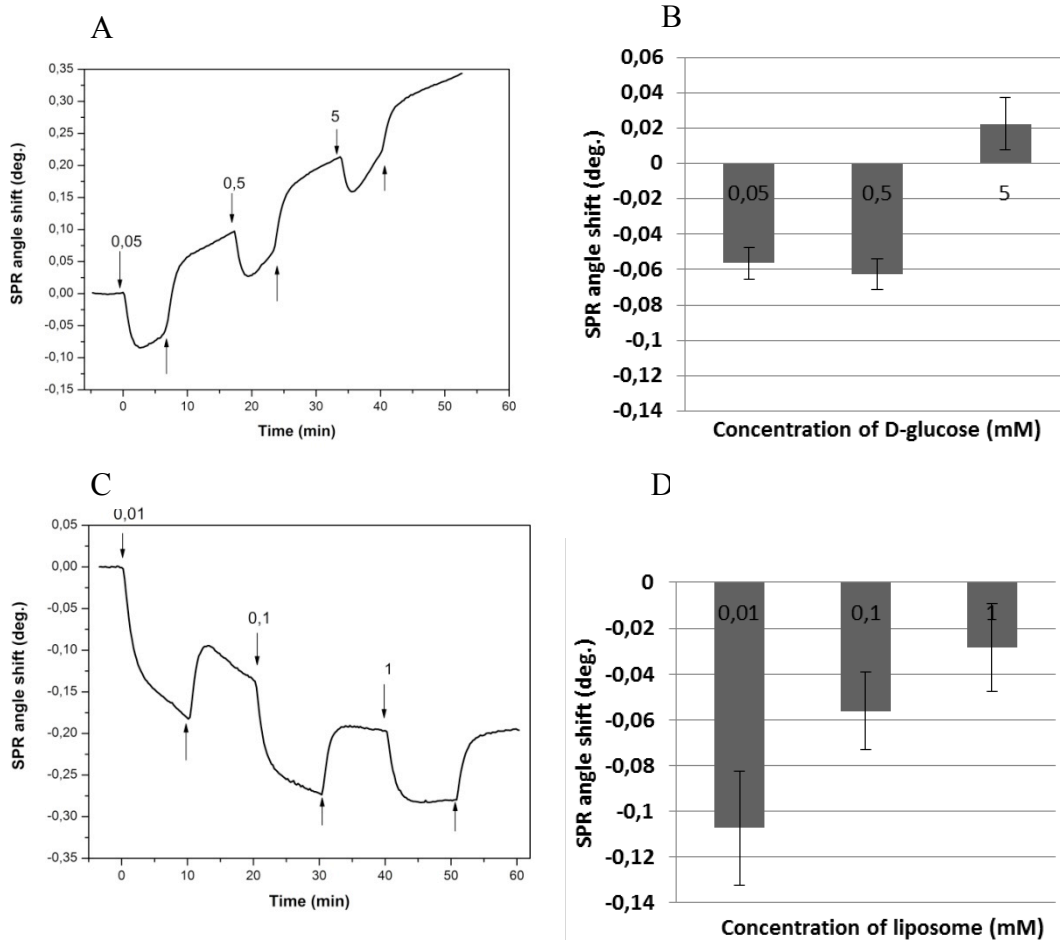


Figure 22. A) Measured changes in the SPR angle as a function of time when the immobilized MDCKII cells were exposed to D-glucose (mM) for 10 min. Down arrows represent the time of sample injections, and up arrows the time of the injection of a pure buffer. B) Maximum measured change in the SPR angle when MDCKII cells were exposed to 0,05; 0,5 and 5 mM D-glucose (n=4). The mean and standard errors of individual measurements are represented. C) Measured changes in the SPR angle as a function of time when the immobilized MDCKII cells were exposed to HSPC:Chol liposomes (mM) for 10 min. D) Maximum measured change in the SPR angle when MDCKII cells were exposed to 0,01; 0,1 and 1 mM HSPC:Chol liposomes (n=4).

Figure 23 compares the SPR signals obtained during exposure of the MDCKII cells to the four different test compounds used in this study. One concentration level of each test compound was plotted in the same graph. As a result, it was found that propranolol and D-glucose induced a similar response, whereas D-mannitol and HSPC:Chol liposomes had similarities in their response. Indeed, propranolol and D-glucose induced changes both in the SPR peak minimum intensity and in the SPR angle, while D-mannitol and HSPC:Chol liposomes only induced a change in the SPR angle. These results verify that the differences in the interaction between the test compound and the immobilized

MDCKII cells can be observed by simultaneously monitoring the changes in both the SPR angle and the SPR peak minimum intensity.

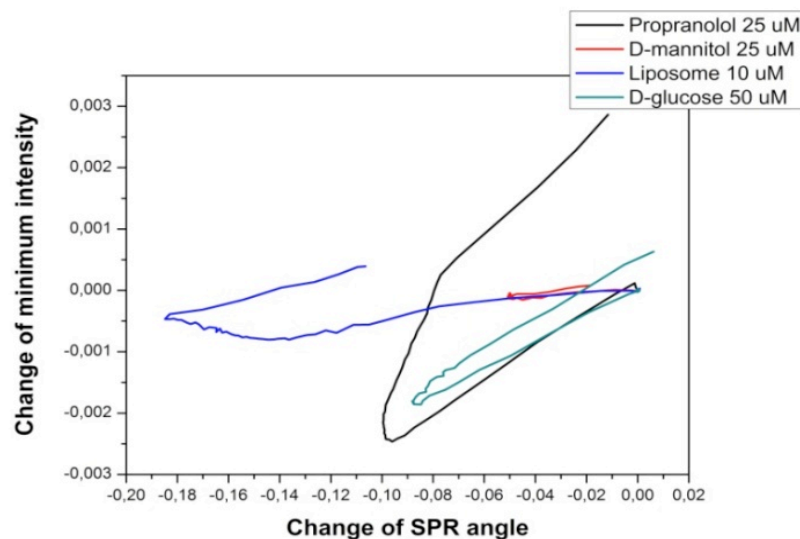


Figure 23. The change in the SPR peak minimum intensity as a function of the change in the SPR angle, when MDCKII cells were exposed to four different test compounds followed by the dissociation in pure buffer.

5 DISCUSSION

5.1 Growing of the cells on PDMS substrates

ARPE-19 cells were grown on the PDMS substrates to study if it would be possible to culture this cell line on the PDMS molded flow channel of the SPR instrument. PDMS is biocompatible, but it is also a hydrophobic material (Wang et al. 2009; Lee et al. 2004). It is generally known that hydrophobic substrates do not promote cell adhesion to the surface (Faucheux et al. 2004). Therefore ARPE-19 cells were not attaching to the PDMS substrates with a common 10:1 elastomer to curing agent mixing ratio. Krishna et al. (2007) have shown that unmodified PDMS does not support the attachment of ARPE-19 cells as good as polystyrene and Klenkler et al. (2005) reported that the epithelial cells did not grow as a confluent monolayer on this material. Similar results have also been obtained with Caco2-cells (Wang et. al 2009).

In order to improve the cell adhesion properties, PDMS substrates were treated with fibronectin, laminin, type I collagen and PLL. The attachment of ARPE-19 cells appeared to be highly dependent on the modification treatment. The micrographs and the viability test revealed that the most confluent and viable ARPE-19 cells were growing on the fibronectin-treated PDMS. Moreover, Liam et al. (2004) have successfully used fibronectin to increase the attachment of ARPE-19 cells on PDMS surfaces. Fibronectin, laminin and type I collagen are all fibrous proteins in the extracellular matrix, which are controlling the cell behavior in a native environment having both structural and adhesive functions (Folch and Toner 2000). However, Gugutkov et al. (2009) have suggested that fibronectin significantly enhances the attachment and proliferation of the cells on PDMS substrates, because its adsorption is higher on a hydrophobic surface than on a wettable surface. Moreover, fibronectin is relatively non-specific in promoting cell adhesion when laminin e.g. has more specificity towards a certain cell type (Carlsson et al. 1981). As the work progressed it became clear that visualizing ARPE-19 cells on the PDMS molded flow channel of the SPR instrument was too difficult (Figure 8). However, it was found that ARPE-19 cells could adhere directly on the surface of non-treated gold sensor chips. Therefore, the more straightforward process of seeding the cells directly on the non-treated gold sensor chips was selected for the SPR measurements. However, the preliminary results concerning the adhesion properties of the ARPE-19 cells on the PDMS molded flow channel of the SPR instrument may be valuable for future studies developing e.g. for developing a flow channel cell culture protocol for SPR analysis.

5.2 Growing and viability of the cells on gold sensor chip

Prior to SPR measurements, the cell culture conditions were optimized in order to grow the cells as a confluent monolayer on the gold sensor chips. The confluence of the immobilized cells was vital because Ziblat et al. (2006) have shown that the surface coverage of cells on the gold sensor chip has a dramatic effect on the shape of the full SPR angle curve. Therefore, in order to obtain repeatable SPR measurements and avoid unspecific interactions of the test compounds not originating from cell interactions, it is

important to develop a cell immobilization protocol that enables a repeatable culture of confluent monolayers on the SPR sensor chip. It was found that both ARPE-19 cells and MDCKII cells attached and proliferated as a confluent monolayer on the non-treated gold sensor chips when compared to fibronectin-treated gold sensor chips and the polystyrene (used as a reference cell culture material). Therefore, it was concluded that no adhesion promoter was required (Figure 9 and 11). Cells have been cultured on non-treated gold sensor chips in also in previous SPR cell studies. Used cell lines included human melanoma (Yashunsky et al. 2009), human basophilic KU812 (Fujimura et al. 2008), RBL-2H3 rat mast and PAM212 mouse keratinocyte cells (Yanase et al. 2007), to name a few. Moreover, Robelek and Weger (2010) have immobilized MDCKII cells directly on the gold sensor chip as a confluent monolayer to study the volume changes of cells.

After reaching confluence, MDCKII cells started to form clusters on the smooth non-treated gold sensor chip surface. Based on microscope visualization it seemed that liquid had gathered under the cells at the clustering points. Cells are generally attached to the surfaces in focal, close, and extracellular matrix contacts, each with its own characteristic separation distance from the surface (Chen and Singer 1982). As a result, cell plasma membranes are normally 10-100 nm away from the substrate surface depending on cell types and culturing conditions, but due to the cluster formation the plasma membranes could have been even further away in those zones in the case of MDCKII cells in this study. The detectable evanescent field of an SPR instrument is approximately 300 nm from the gold sensor chip surface and the height of cells is in the micrometer range meaning that some of the cells may have been out of the evanescent field due to the cluster formation. Therefore, those clusters may influence on the SPR results. However, this effect was minimized as much as possible by optimizing the seeding density. Trypan blue and MTT test showed that the non-treated gold sensor chip surface is not cytotoxic for ARPE-19 cells or MDCKII cells.

5.3 Resistance of cells to buffer flow

The results from the flow experiments with the immobilizer demonstrated that MDCKII cells were able to resist shear stress induced by buffer flow much better than ARPE-19 cells. This can probably be explained by the physiological location of the cells. ARPE-19 cell line has been derived from the normal eyes of a 19-year-old male where the cells constitute a monolayer between the choroid and the neurosensory retina, while the MDCKII cell line has been derived from the distal tubule or the collecting duct of the nephron of a canine. The parameters that influence the shear stress are flow, radius and medium viscosity (Reneman et al. 2006). The blood flow in a 70 kg young healthy adult in kidneys is approximately 1240 ml/min while the blood flow in a human retina has been measured to be $0,261 \pm 0,087$ ml/min (Maleki et al. 2010; Davies and Morris 1993). The shear stress is significantly higher in blood vessels in kidneys compared to the eye so it may be the reason why MDCKII tolerated the shear stress induced by buffer flow better than ARPE-19 cells. Moreover, these cell lines may also have differences in how strongly they interact with the gold surface, which can influence the ability of the cells to resist the buffer flow. The results indeed suggest that MDCKII cells adhere more strongly to the surface of the non-treated gold sensor chip than ARPE-19 cells. The flow experiments also indicated that when the cells were cultured a longer period than one day, the cells adhered stronger to the surface of the non-treated gold sensor chip and could better resist the shear stress induced by buffer flow.

5.4 Surface plasmon resonance in living cell sensing

The dominant SPR application for the past 20 years has been to measure different protein-protein and other biomolecular interactions in real-time without labeling (Rich and Myszka 2010; De Crescenzo et al. 2008). Traditionally, this has been done by measuring only changes in the SPR angle as a function of time. In this work not only the change in the SPR angle but also the change in the SPR peak minimum intensity was measured in order to further clarify if SPR is able to distinguish between differences in the interactions the test compounds and the immobilized MDCKII cells. The aim of this work was to study the suitability ability of the SPR technique to monitor

drug-cell interactions when cells were directly immobilized on the gold sensor chip. It was observed that the immobilized MDCKII cells induced rapid changes in the SPR angle when the cells were exposed to increasing concentrations of propranolol, D-mannitol, D-glucose or HSPC:Chol liposomes. The change in the SPR angle showed that the immobilized cells were reacting to external stimuli. It should be noted that the detectable evanescent field on the gold sensor chip is approximately 300 nm, while the thickness of the MDCKII cell monolayer is approximately 6 μm meaning that the distance between the stimulated cell surface and the gold sensor chip surface is far longer than the detectable range (Kersting et al. 1993). The observed change in the SPR angle is therefore mainly due to the cellular response and the surface adsorption does not have a significant influence on the measured change in the SPR angle. For this reason, the transport process in the cell surface itself cannot be detected by the SPR instrument. The transport process still triggers intracellular mass redistribution, e.g. calcium mobilization or cytoskeleton remodeling, and these changes may generate a change in the SPR signal (Kholodenko 2003).

The exposure of MDCKII cells to several concentrations of propranolol or D-mannitol caused a significant change in the SPR angle (Figure 18A and 20A). However, no significant change in the SPR angle was measured when propranolol or D-mannitol was allowed to interact with a no-treated gold sensor chip without the cells (Figure 18C and 20C). As a result, this confirms that the measured change in the SPR angle during the interaction of the test compounds with the immobilized MDCKII cells actually shows real drug-cell interactions and not drug-gold interactions. This is true, because when a cell monolayer is present on the surface of the gold sensor chip then most of the sensor surface is not accessible to the test compound and this limits the contribution of a bulky effect by the test compound to a relatively small proportion of the total sensor area. Previously, Robelek and Wegener (2010) demonstrated in their study that the measured SPR signal reflects the cellular reactions of the immobilized MDCKII cells, and not a simple change in the bulk refractive index when the cells are stimulated with a test compound. They rinsed the gold sensor chip without the cells, and cell-covered gold sensor chip with 10% polyvinylpyrrolidone in the running buffer to raise the bulk refractive index substantially without influencing buffer osmolarity. As a result, they

observed a radical signal shift with the gold sensor chip without the cells whereas the cell-covered gold sensor chip induced only a minor, very prolonged SPR signal change.

The measured change in the SPR angle was negative for each concentration of propranolol and D-mannitol except for 250 μM propranolol for which it was positive (Figure 18 and 20). It is generally known that propranolol diffuses effectively by the transcellular pathway into cells, whereas D-mannitol uses the paracellular pathway (Salama et al. 2003; Polli et al. 2001). It was surprising that the exposure to D-mannitol induced a negative change in the SPR angle. It was expected that no change in the SPR angle should be observed because D-mannitol is not readily diffused into the cells. On the other hand, it was expected that propranolol induces a positive change in the SPR angle because propranolol should readily diffuse into the cells. A widely accepted simplification for the measured SPR signal is that the SPR angle is linearly proportional to the mass change in the evanescent field. It has been suggested in the literature that when cells are immobilized on the gold sensor chip of an SPR instrument, a shift in the SPR angle also correlates with the mass redistribution within the cells and not only the mass accumulation of the test compound within the cells (Yanase et al. 2007; Fang et al. 2006). This mass redistribution is a sum of all redistribution events within the evanescent field occurring at different distances away from the surface of the gold sensor chip. The mass redistribution could indeed induce either negative or positive changes in the measured SPR angle depending on if the intracellular mass migration within the cells is in the direction away from or towards the SPR evanescent field during the exposure of the test compound. Based on these results, the negative changes in the SPR angle with propranolol and D-mannitol would suggest that the exposure induced a mass redistribution away from the evanescent field in both cases.

Only the highest concentration of propranolol (250 μM) induced first a negative shift accompanied with a major positive shift in the SPR angle (Figure 18) indicating that first propranolol initially induced a mass redistribution away from the evanescent field followed by a mass redistribution towards the evanescent field. This result suggests that when the immobilized MDCKII cells are exposed to a low concentration of propranolol it induces a cell contraction followed by mass redistribution away from the evanescent

field, which is observed as a negative change in the SPR angle. However, the highest concentration of propranolol will induce both a mass redistribution and/or morphological changes towards the evanescent field and an accumulation of propranolol within the cells. Consequently, a positive change in the SPR angle during the exposure is not observed at low concentrations of propranolol because the amount of absorbed propranolol is not sufficient to render the SPR angle positive. Similar behavior has been illustrated for HEK-293 cells stimulated with angiotensin II by verifying the results with phase-contrast microscopy imaging (Cuerrier et al. 2008). This is also further supported by the studies by Yashunsky et al. (2009). Cuerrier et al. (2008) showed that the contraction of cells induces a negative SPR shift in the fixed angle intensity, while Yashunsky et al. (2009) showed that the cell spreading induces an increase in the fixed angle intensity with mid infra-red SPR. Based on the discussion above, the negative change in the SPR angle when the immobilized MDCKII cells were exposed to propranolol, D-mannitol, D-glucose and HSPC:Chol liposomes may be an indication of a cell contraction induced by the test compound.

All SPR studies in the literature involving the immobilization of cells on the gold sensor chip only monitors the change either in the SPR angle or the intensity change at a fixed angle near the minimum of the SPR peak, and none has observed that together with the change in the SPR peak minimum intensity (Chabot et al. 2009; Fujimura et al. 2008; Yanase et al. 2007). When comparing the measured change in the SPR peak minimum intensity between propranolol and D-mannitol, only the exposure to propranolol changed the SPR peak minimum intensity (Figure 21). Propranolol induced a negative change in the SPR peak minimum intensity at low concentrations, but for the highest concentration it was positive. In other words, the propranolol induced a change in both the SPR angle and the SPR peak minimum intensity, while D-mannitol induced only a change in the SPR angle. Based on these results, it is clear that the stimulation with a drug, which diffuses into cells transcellularly, induces a change in both the SPR angle and the SPR peak minimum intensity, while a drug which is absorbed paracellularly induces only a change in the SPR angle. These results indicate that when the immobilized MDCKII cells are exposed to propranolol it triggers intracellular mass redistribution within the cells, while D-mannitol does not. Because the SPR peak

minimum intensity changed only in the case of propranolol, these findings strongly suggest that the change in the SPR angle indicates cell contraction (a negative change) or cell spreading (a positive change), while the change in the SPR peak minimum intensity reveals the accumulation/depletion of the test compound and/or the intracellular mass redistribution within the cells.

The discussion above is supported by the observation that D-glucose which is transported via carriers into the cells also induced a change in the SPR peak minimum intensity, while HSPC:Chol liposomes produced only a minor change (Figure 23). The liposomes are actively transported into cells by endocytosis, but the interaction time (maximum 10 min) between the immobilized MDCKII cells and HSPC:Chol liposomes was probably too short for the endocytosis to take place (Lee et al. 1993). The process of liposomal uptake is a two-step process consisting of liposome binding to cell surface sites followed by endocytosis (Miller et al. 1998). Due to a short analysis time, only the cell response induced by interaction between liposomes and the cell surface could be detected by the SPR instrument.

Moreover, it was shown that after the exposure of propranolol the baseline was shifted to a higher value when both the SPR angle and the SPR peak minimum intensity was observed. In the case of D-mannitol the baseline of the SPR angle and the SPR peak minimum intensity basically returned to the same level as before exposure. These results also supports the finding that during the exposure of MDCKII cells to propranolol, it was readily diffused transcellularly into the immobilized cells, and after the exposure a part of the accumulated propranolol remained in the cells increasing the baseline level. Clearly, the accumulation of D-mannitol within the cells was not observed because D-mannitol is transported by a paracellular pathway (Salama et al. 2003). This is also supported by the fact that the change in the SPR angle was basically constant for all concentration and much smaller in the case of D-mannitol compared to propranolol. In addition, as illustrated in Figure 22, the increase in the baseline of the measured SPR angle after the exposure was also observed when MDCKII cells were exposed to D-glucose, which is transported into cells via transporters (Wang et al. 1997). However, any quantitative analysis of these results was not possible at the time

of the studies due to the lack of proper analysis tools. However, the results from this study combined with further drug-cell interaction studies with SPR could in the future allow for the development of proper tools for quantitative analysis of the SPR responses in living cell sensing.

It should be mentioned that in this work, there was a clear variation in the results of the SPR measurements. The SPR angular scan changed when MDCKII cells with a higher passage number were used in the measurements. The SPR measurements in this work were done with passage number 15-29 for MDCKII cells. In the first measurements, the results were more repeatable than in those that were performed later. Based on the results, it is practical to use only lower passage numbers of MDCKII cells in the cell-based assays with optical biosensors. The SPR peak minimum intensity and the SPR angle are sensitive to the cell density and viability meaning that the biological status of cells, e.g. cell viability, cell density and degree of adhesion, can significantly influence the results and cause assay variability (Horvath et al. 2001). In the measurements in this study, the confluence of the cell monolayer on the gold sensor chip was ensured by the flow experiments and microscopic visualizations before each measurement. However, when MDCKII cells were grown as a confluent monolayer on the non-treated gold sensor chips, the cells were often forming clusters despite the attempt to optimize the cell culture conditions, which could have an effect on the SPR signals. Moreover, the optical signal can be dependent on the cell states (Fang et al. 2005). If cells are in a proliferating state, the response of the cells to the stimulation with a test compound may be different and therefore induce assay variability. It is clear that further studies with several drugs are required that reliable conclusions can be drawn. It may be advantageous in the future to perform the SPR measurements with one concentration level at a time and allow the test compound and the immobilized cells to interact for a longer period of time. This may facilitate a better quantitative and not only qualitative the interpretation of the results.

6 CONCLUSIONS

This study shows that SPR has the capacity to determine cellular activity in real-time when cells immobilized on the SPR sensor chip are stimulated with various agents. MDCKII and ARPE-19 cells can be cultured on the gold sensor chip, but only MDCKII cells can resist harsh conditions, such as flow and ambient temperature, during the SPR measurements. This indicates that the cell type used need to be firmly attached to the sensing surface. The results show that when both the change in the SPR angle and the SPR peak minimum intensity are simultaneously monitored it improves the mechanistic understanding of the SPR responses in living cell sensing compared to cases when only the changed in the SPR angle is monitored. The approach demonstrated in this work also enables to differentiate between the type and modes of drug actions when monitoring drug-cell interactions by SPR. This was clearly demonstrated by using two drugs that utilizes different absorption pathways as test compounds, i.e. propranolol (transcellular) and D-mannitol (paracellular). Hence, SPR may be a potential *in vitro* method in order to provide real-time complementary information on the permeability of drugs and possibly also about cell uptake mechanisms of nanoparticles for traditional *in vitro* cell assays for a better mechanistic understanding of drug-cell interactions on a cellular level.

7 REFERENCES

Chabot V, Cuerrier CM, Escher E, Aimez V, Grandbois M, Charette PG: Biosensing based on surface plasmon resonance and living cells. *Biosens Bioelectron* 24: 1667–1673, 2009

Chen WT, Singer SJ: Immunoelectron microscopic studies of the sites of cell-substratum and cell-cell contacts in cultured fibroblasts. *J Cell Biol* 95: 205-222, 1982

Cuerrier CM, Chabot V, Vigneux S, Aimez V, Escher E, Gobeil F, Charette PG, Grandbois M: Surface plasmon resonance monitoring of cell monolayer integrity: Implication of signaling pathways involved in actin-driven morphological remodeling. *Cell Mol Bioeng* 1: 229-239, 2008

Davies B, Morris T: Physiological parameters in laboratory animals and humans. *Pharm Res* 10: 1093-1095, 1993

De Crescenzo G, Boucher C, Durocher Y, Jolicoeur M: Kinetic characterization by surface plasmon resonance-based biosensors: Principle and emerging trends. *Cell Mol Bioeng* 1: 204–215, 2008

Fang Y: The development of label-free cellular assays for drug discovery. *Expert Opin Drug Discov* 6:1285-1298, 2011

Fang Y, Ferrie AM, Fontaine NH, Mauro J, Balakrishnan J: Resonant waveguide grating biosensor for living cell sensing. *Biophys J* 91: 1925–1940, 2006

Fang Y, Li G, Peng J: Optical biosensor provides insights for bradykinin B2 receptor signaling in A431 cells. *Febs Lett* 579: 6365-6374, 2005

Faucheux N, Schweissb R, Lutzowa, Wernerb KC, Grotha T: Self-assembled monolayers with different terminating groups as model substrates for cell adhesion studies. *Biomaterials* 25: 2721–2730, 2004

Folch A, Toner M: Microengineering of cellular interactions. *Annu Rev Biomed Eng* 2: 227–56, 2000

Fujimura Y, Umeda D, Yamada K, Tachiban H: The impact of the 67 kDa laminin receptor on both cell-surface binding and anti-allergic action of tea catechins. *Arch Biochem Biophys* 476: 133–138, 2008

Gugutkov D, Altankov G, Rodriguez Hernandez JS, Pradas MM, Sanchez MS: Fibronectin activity on substrates with controlled -OH density. *J Biomed Mater Res* 92A: 322–331, 2010

Horvath R, Vörös J, Graf R, Fricsovszky G, Textor M, Lindvold RL, Spencer ND, Papp E: Effect of patterns and inhomogeneities on the surface of waveguides used for optical waveguide lightmode spectroscopy applications. *Appl Phys B*72: 441–447, 2001

Hämäläinen MD, Markgren P-O, Schaal W, Karlen A, Classon B, Vrang L, Samuelsson B, Hallberg A, Danielson UH: Characterization of a set of HIV-1 protease inhibitors using binding kinetics data from a biosensor-based screen. *J Biomol Screen* 5: 353-359, 2000

Kersting U, Schwab A, Treidtel M, Pfaller W, Gstraunthaler G, Steigner W, Oberleithner H: Differentiation of Madin-Darby canine kidney cells depends on cell culture conditions. *Cell Physiol Biochem* 3: 42–55, 1993

Kholodenko BN: Four-dimensional organization of protein kinase signaling cascades: the roles of diffusion, endocytosis and molecular motors. *J Exp Biol* 206: 2073-2082, 2003

Klenkler BJ, Griffith M, Becerril C, West-Mays JA, Sheardown H: EGF-grafted PDMS surfaces in artificial cornea applications. *Biomaterials* 26: 7286–7296, 2005

Kooyman RPH: Physics of surface plasmon resonance. *Handbook of Surface Plasmon Resonance*, p.15-34, Edited by Schasfoort RBM, Tudos AJ, The Royal society of Chemistry, Cambridge 2008

Krishna Y, Sheridan CM, Kent DL, Grierson I, Williams RL: Polydimethylsiloxane as a substrate for retinal pigment epithelial cell growth. *J Biomed Mater Res* 80A: 669-678, 2007

Lee JN, Jiang X, Ryan D, Whitesides GM: Compatibility of mammalian cells on surfaces of poly(dimethylsiloxane). *Langmuir* 20: 11684-11691, 2004

Lee KD, Nir S, Papahadjopoulos D: Quantitative analysis of liposome-cell interactions in vitro: rate constants of binding and endocytosis with suspension and adherent. *Biochemistry* 32: 889-899, 1993

Liang H, Miranto H, Granqvist N, Sadowski JW, Viitala T, Wang B, Yliperttula M: Surface plasmon resonance instrument as a refractometer for liquids and ultrathin films. *Sensor Actuator B* 149: 212–220, 2010

Lim JM, Byun S, Chung S, Park TH, Seo JM, Joo CK, Chung H, Cho D: Retinal pigment epithelial cell behavior is modulated by alterations in focal cell–substrate contacts. *Invest Ophthalmol Vis Sci* 45: 4210-4216, 2004

Maleki N, Dai W, Alsop DC: Blood flow quantification of the human retina with MRI. *NMR biomed* 24: 104 -111, 2010

Miller CM, Bondurant B, McLean SD, McGovern KA, O'Brien DF: Liposome-cell interactions in vitro: Effect of liposome surface charge on the binding and endocytosis of conventional and sterically stabilized liposomes. *Biochemistry* 37: 12875-12883, 1998

Polli JW, Wring SA, Humphreys JE, Huang L, Morgan JB, Webster LO, Serabjit-Singh CS: Rational use of *in vitro* P-glycoprotein assays in drug discovery. *J Pharmacol Exp Ther* 299: 620-628, 2001

Reneman RS, Arts T, Hoeks APG: Wall shear stress – an important determinant of endothelial cell function and structure in the arterial system *in vivo*. *J Vasc Res* 43: 251–269, 2006

Rich RL, Myszka DG: Grading the commercial optical biosensor literature - Class of 2008: 'The Mighty Binders'. *J Mol Recognit* 23: 1-64, 2010

Rezania A, E. Healy KA: Biomimetic peptide surfaces that regulate adhesion, spreading, cytoskeletal organization, and mineralization of the matrix deposited by osteoblast-like cells. *Biotechnol Prog* 15: 19-32, 1999

Robelek R, Wegener J: Label-free and time-resolved measurements of cell volume changes by surface plasmon resonance (SPR) spectroscopy. *Biosens Bioelectron* 25: 1221–1224, 2010

Salama NN, Fasano A, Lu R, Eddington ND: Effect of the biologically active fragment of zonula occludens toxin, ΔG , on the intestinal paracellular transport and oral absorption of mannitol. *Int J Pharm* 251: 113-121, 2003

Tudos JT, Schasfoort RBM: Introduction to surface plasmon resonance. *Handbook of Surface Plasmon Resonance*, p.5, Edited by Schasfoort RBM, Tudos AJ, The Royal society of Chemistry, Cambridge 2008

Yanase Y, Suzuki H, Tsutsui T, Hiragun T, Kameyoshi Y, Hide M: The SPR signal in living cells reflects changes other than the area of adhesion and the formation of cell constructions. *Biosens Bioelectron* 22: 1081–1086, 2007

Yashunsky V, Shimron S, Lirtsman V, Weiss AM, Melamed-Book N, Golosovsky M, Davidov D, Aroeti B: Real-time monitoring of transferrin-induced endocytic vesicle formation by mid-infrared surface plasmon resonance. *Biophys J* 97: 1003–1012, 2009

Yavin E, Yavin Z: Attachment and culture of dissociated cells from rat embryo cerebral hemispheres on polylysine-coated surface. *J Cell Biol* 62: 540-546, 1974

Viitala T, Liang H, Gupta M, Zwinger T, Yliperttula M, Bunker A: Fluid dynamics modeling for synchronizing surface plasmon resonance and quartz crystal microbalance as tools for biomolecular ant targeted drug deliver studies. *J Colloid Interf Sci* 378: 251-259, 2012

Wang L, Sun B, Ziemer KS, Barabino GA, Carrier RL: Chemical and physical modifications to poly(dimethylsiloxane) surfaces affect adhesion of Caco-2 cells. *J Biomed Mater Res* 93A: 1260-1271, 2009

Wang Y, Aun R, Tse LSF: Absorption of D-glucose in the rat studied using in situ intestinal perfusion: A permeability index approach. *Pharmaceut res* 14: 1563-1567, 1997

Ziblat R, Lirtsman V, Davidov D, Aroeti B: Infrared surface plasmon resonance: A novel tool for real-time sensing of variations in living cells. *Biophys J* 90: 2592–2599, 2006